

# Segmenting Human–LLM Co-authored Text via Change Point Detection

Mengchu Li<sup>1\*</sup>; Jin Zhu<sup>1\*</sup>, Jinglai Li<sup>1</sup>, Chengchun Shi<sup>2,†</sup>

<sup>1</sup>School of Mathematics, University of Birmingham

<sup>2</sup>Department of Statistics, London School of Economics and Political Science

## Abstract

The rise of large language models (LLMs) has created an urgent need to distinguish between human-written and LLM-generated text to ensure authenticity and societal trust. Existing detectors typically provide a binary classification for an entire passage; however, this is insufficient for human–LLM co-authored text, where the objective is to localize specific segments authored by humans or LLMs. To bridge this gap, we propose algorithms to segment text into human- and LLM-authored pieces. Our key observation is that such a segmentation task is conceptually similar to classical change point detection in time-series analysis. Leveraging this analogy, we adapt change point detection to LLM-generated text detection, develop a weighted algorithm and a generalized algorithm to accommodate heterogeneous detection score variability, and establish the minimax optimality of our procedure. Empirically, we demonstrate the strong performance of our approach against a wide range of existing baselines.

## 1 Introduction

State-of-the-art large language models (LLMs), including GPT-5 (OpenAI, 2025), Gemini (Comanici et al., 2025), and Grok-4 (xAI, 2025), exhibit strong capabilities in following human instructions, performing complex reasoning, and generating text at scale. These powerful tools have been deeply integrated into both professional and daily workflows, rendering LLM-generated content pervasive across various domains, such as academic literature, technical reports, and student assignments. This growth has spurred a line of research on LLM-generated text detection; see Section 1.1 for a review.

These works typically study detection as a binary classification problem, determining whether an entire passage is human- or LLM-authored. However, in practice, LLM-generated text is rarely used without modification. Users often revise, edit, or blend it with their own writing. For instance, in technical reports, users may draft the core methodological sections themselves while relying on LLMs to generate descriptive text for tables and figures. In creative writing, authors may collaboratively generate stories with LLMs (Xie et al., 2023). Such human–LLM co-authoring settings have become increasingly common as LLMs continue to evolve.

---

\*Equal contribution. †Corresponding author.

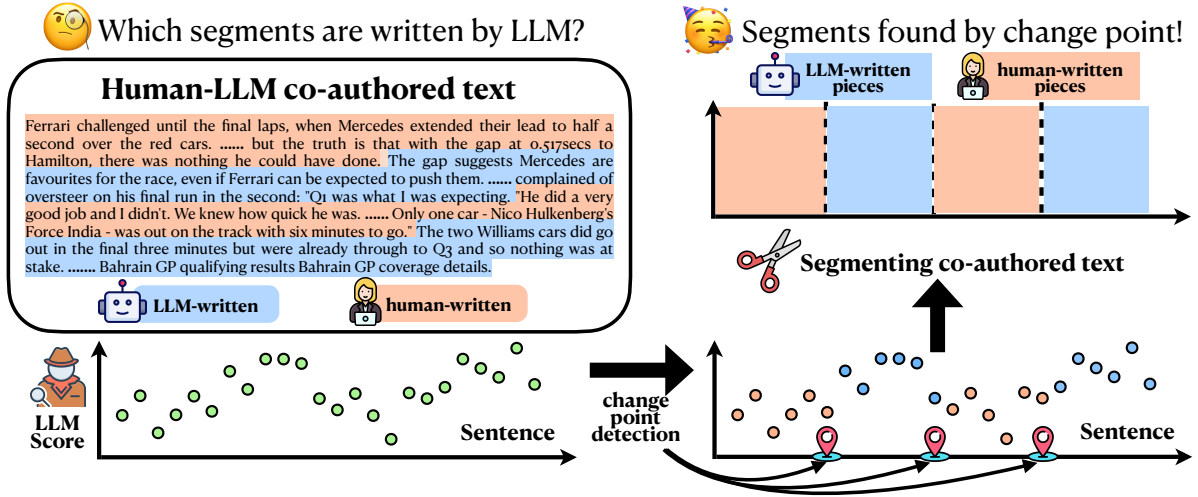


Figure 1: Workflow of our proposal, which adapts change point detection to LLM-generated text localization.

In these “hybrid” settings, a binary classification of an entire passage as human- or LLM-authored is insufficient. A more meaningful question is whether we can segment the document into human- and LLM-authored pieces to identify which portions are generated by LLMs. However, as discussed in Section 1.1, only a few works have considered LLM-generated text localization.

This paper advances the state of LLM text detection by making the following **contributions**:

- We identify that the problem of segmenting human–LLM co-authored text is conceptually closely connected to *change point detection* problems in time-series analysis. This perspective motivates a new framework that adapts change point detection for LLM-generated text localization (refer to Figure 1 for a graphical visualization of the workflow).
- We propose three change point detection algorithms tailored to human–LLM text segmentation. We begin with a *vanilla* adaptation of classical change point detection (Section 3.1) and reveal its limitations in settings with heterogeneous detection score variability. To overcome this limitation, we develop a *weighted* algorithm (Section 3.2) and a *generalized* algorithm (Section 3.3) that encode sentence-specific information and substantially improve segmentation accuracy.
- We derive *estimation error bounds* for both vanilla and weighted algorithms (Theorems 1 and 2), showing that the latter achieves more accurate estimation under less restrictive signal-to-noise ratio conditions. Together with a *minimax lower bound* that characterizes the intrinsic difficulty of the segmentation problem (Theorem 3), we demonstrate that the weighted algorithm achieves this limit, establishing its *minimax optimality*. We further extend such optimality guarantees to the generalized algorithm under appropriate conditions.
- We evaluate the empirical performance of the proposed algorithms across a broad range of experimental settings (Section 5 and Appendix B). Results demonstrate that our proposal consistently outperforms existing baseline algorithms, reducing segmentation errors by up to 50%.

## 1.1 Literature review

Our proposal is closely related to three main bodies of literature: LLM-generated text detection, LLM-generated text localization, and change point detection in time-series analysis.

**LLM-generated text detection.** These works primarily study the binary classification problem of distinguishing between human- and LLM-authored text. Existing approaches can be broadly categorized into machine learning (ML)-based and zero-shot methods. Specifically, ML-based methods collect datasets of human-written text, prompt LLMs to produce corresponding rewrites, and then utilize both sources of text to train a classifier to perform this binary classification (Solaiman et al., 2019; Ippolito et al., 2020; Guo et al., 2023; Hu et al., 2023; Mao et al., 2024; Guo et al., 2024; Tian et al., 2024; Yu et al., 2024; Chen et al., 2025; Zhou et al., 2025, 2026b). In contrast, zero-shot methods are training-free. They construct statistical measures derived directly from the text, such as its intrinsic dimensionality, or based on the next-token probability distributions of a target LLM (Gehrmann et al., 2019; Mitchell et al., 2023; Su et al., 2023; Tulchinskii et al., 2023; Bao et al., 2024; Hans et al., 2024; Yang et al., 2024; Song et al., 2025). These measures take on different values for human and LLM-authored content, which serves as the basis for classification.

While our proposal employs similar techniques for distinguishing between human and LLM-generated text, we study the more complex problem of text localization rather than providing a binary label for the entire passage, as discussed below.

**LLM-generated text localization.** In practical settings, users rarely adopt LLM-generated text directly. Instead, they revise or edit the generated content (Zhang et al., 2024a). This collaborative writing process is commonly referred to as *human-AI co-authoring*. LLM-generated text localization aims to localize the portions of a document that originate from an LLM. Dugan et al. (2023) empirically evaluate humans’ ability to detect the boundary between human- and LLM-authored text. A line of recent research applies existing detectors at the sentence level to localize LLM-authored sentences (Wang et al., 2023; Zeng et al., 2024b; Jiang et al., 2025). In contrast, Su et al. (2025) adopt a bottom-up approach, performing token-level detection and aggregating these classifications to determine whether a sentence is authored by a human or an LLM. In addition to these works, Zhang et al. (2024b) demonstrate that pooling information across several consecutive sentences improves performance over individual sentence-level classification. Li et al. (2024) combine standard change point algorithms with watermarking techniques to obtain text segmentation.

**Change point detection.** Change point detection aims to identify and localize structural changes within a sequence of observations – for instance, a sudden shift in their expected value. It has been a popular research topic in statistics and machine learning (e.g., Baranowski et al., 2019; Verzelen et al., 2023; Bhattacharyya & Ramdas, 2025; Wang et al., 2020). The literature on change point detection covers different types of data and various categories of structural changes. Methodologically, the CUSUM statistic, introduced in Section 2.2, plays a central role in numerous algorithms (e.g. Fryzlewicz, 2014; Baranowski et al., 2019; Wang et al., 2020; Cho & Kirch, 2022; Wang et al., 2021). Theoretically, minimax rates of convergence have been

established to understand the fundamental difficulty of different problems and to provide a rigorous benchmark for evaluating different algorithms (e.g. Yu, 2020).

## 2 Preliminaries

We first introduce examples of detection statistics for LLM-generated text, the CUSUM statistic and the Narrowest-Over-Thresholding (NOT, Baranowski et al., 2019) algorithm for classical change point detection, upon which our proposal is built. Next, we formulate our problem of text segmentation/localization and discuss its connection to change point detection.

### 2.1 Detection statistics for LLM-generated text

While our framework allows the use of general detection statistics, we consider, for illustration purposes, the zero-shot FastDetectGPT (Bao et al., 2024) statistic, which leverages the next-token prediction probabilities from a pre-trained language model. Given a text segment  $\mathbf{Z}$  containing  $n$  tokens, let  $\mathbf{Z}_{<t} := (Z_1, Z_2, \dots, Z_{t-1})$ . Consider the following detection statistic:

$$\phi(\mathbf{Z}) = \frac{1}{n} \sum_{t=1}^n \left\{ \log \text{score}(Z_t | \mathbf{Z}_{<t}) - \mathbb{E}_{Z'_t \sim \text{sample}(\bullet | \mathbf{Z}_{<t})} [\log \text{score}(Z'_t | \mathbf{Z}_{<t})] \right\},$$

where  $\text{score}(\bullet | \mathbf{Z}_{<t})$  denotes the scoring model and  $\text{sample}(\bullet | \mathbf{Z}_{<t})$  denotes the sampling model, which is used to sample  $Z'_t$  given  $\mathbf{Z}_{<t}$ , and which may be different from the scoring model. The intuition behind this statistic is that LLM-generated text tends to yield higher values compared to human-written text. We also note that the variance of  $\phi(\mathbf{Z})$  when  $\mathbf{Z}$  is generated from the sampling model can be approximated by  $\hat{\sigma}^2(\mathbf{Z}) = n^{-2} \sum_t \text{Var}_{Z'_t \sim \text{sample}(\bullet | \mathbf{Z}_{<t})} [\log \text{score}(Z'_t | \mathbf{Z}_{<t})]$ . It is clear from the formulation that as the length of the text  $n$  increases, the variability of  $\phi(\mathbf{Z})$  tends to decrease and therefore becomes more reliable. Further developments based on FastDetectGPT utilize training data to improve performance (e.g. Zhou et al., 2025, 2026a), and we consider those ML-based variants in our experiments as well.

### 2.2 CUSUM and NOT for change point detection

Let  $\mathbf{Y} = (Y_1, \dots, Y_N)$  denote a time series of  $N$  observations indexed sequentially. The goal of change point detection is to identify structural changes within this sequence. For example, letting  $\mu_i = \mathbb{E}(Y_i)$  represent the expected value of each observation, we seek to determine the locations  $t$  where  $\mu_t \neq \mu_{t+1}$ . Throughout the rest of the paper, we let  $[N]$  denote the set of integers  $\{1, \dots, N\}$  for  $N \in \mathbb{Z}_+$ .

The CUSUM statistic plays a crucial role in these algorithms. For any time points  $\{s, t, e\} \subset [N]$  such that  $s \leq t < e$ , the CUSUM statistic at  $t$  over the interval  $[s, e]$  is defined as

$$C_{s,e}^{\mathbf{Y}}(t) = \sqrt{\frac{S_{s:t} S_{(t+1):e}}{S_{s:e}}} |\bar{Y}_{s:t} - \bar{Y}_{(t+1):e}|, \quad (1)$$

where  $\bar{Y}_{t_1:t_2}$  denotes the sample average of observations  $\{Y_t\}_t$  in the interval  $[t_1, t_2]$  and  $S_{t_1:t_2} = t_2 - t_1 + 1$  denotes the number of samples within  $[t_1, t_2]$ .

---

**Procedure 1** NOT-meta algorithm

---

**Input:** (i) Data vector  $\mathbf{Y} = (Y_1, \dots, Y_N)$ , (ii) Threshold parameter  $r$ ; (iii) Number of random intervals  $M$ ; (iv) Statistics  $A_{s,e}^{\mathbf{Y}}(b), B(s, e)$

**Output:** Set of estimated change points  $\mathcal{S} \subset \{1, \dots, N\}$ .

- 1: Let  $e \leftarrow N$ ,  $s \leftarrow 1$  and  $\mathcal{S} \leftarrow \emptyset$ , apply **NOT-meta**( $s, e, r$ ) described in Steps 2–15.
  - 2: **if**  $e - s < 1$  **then**
  - 3:   STOP
  - 4: **else**
  - 5:   Uniformly randomly draw  $M$  intervals within  $[s, e]$  and form an interval set  $\mathcal{M}$
  - 6:    $\mathcal{O} \leftarrow \left\{ m \in \mathcal{M} : \max_{s_m \leq b < e_m} A_{s_m, e_m}^{\mathbf{Y}}(b) > r \right\}$
  - 7:   **if**  $\mathcal{O} = \emptyset$  **then**
  - 8:     STOP
  - 9:   **else**
  - 10:      $m^* \leftarrow \arg \min_{m \in \mathcal{O}} B(s_m, e_m), b^* \leftarrow \arg \max_{s_{m^*} \leq b < e_{m^*}} A_{s_{m^*}, e_{m^*}}^{\mathbf{Y}}(b),$
  - 11:      $\mathcal{S} \leftarrow \mathcal{S} \cup \{b^*\}$
  - 12:     **NOT-meta**( $s, b^*, r$ )
  - 13:     **NOT-meta**( $b^* + 1, e, r$ )
  - 14:   **end if**
  - 15: **end if**
- 

It can be shown that  $\max_{s \leq b < e} |C_{s,e}^{\mathbf{Y}}(b)|$  is the generalized likelihood ratio statistic for testing whether there is a change in the sequence  $\{\mu_t\}_t$  under Gaussian assumptions (e.g., [Baranowski et al., 2019](#); [Wang et al., 2020](#)). Beyond the Gaussian case, the applicability of this maximal-type statistic extends to various data distributions as well. It has served as a cornerstone for a wide range of change point detection algorithms with both strong theoretical guarantees and promising empirical performance (e.g., [Liu et al., 2021](#); [Padilla et al., 2021](#); [Wang et al., 2021](#); [Li et al., 2022](#)).

Of particular interest is the NOT algorithm ([Baranowski et al., 2019](#)), which we adapt for our task of LLM text localization. In Algorithm 1, we detail a meta-algorithm that slightly differs from the original NOT algorithm. This version allows two arbitrary statistics,  $A_{s,e}^{\mathbf{Y}}(b)$  and  $B(s, e)$ , as inputs, which can be tailored to our needs. Note that with the default choice  $A_{s,e}^{\mathbf{Y}}(b) = C_{s,e}^{\mathbf{Y}}(b)$ ,  $B(s, e) = e - s$ , Algorithm 1 reduces to the original algorithm.

The main advantage of NOT lies in its ability to accurately localize multiple change points. With multiple change points, their joint effect can make individual changes difficult to detect; see the discussion around Figure 1 of [Fryzlewicz \(2014\)](#). This challenge is addressed by sampling several random intervals in Line 5 of Algorithm 1, which ensures that with high probability, each individual change point is isolated as the only structural change in at least one randomly generated interval, thus facilitating its detection.

### 2.3 Problem setup

Consider a paragraph or an article  $\mathbf{X}$  partitioned into  $N$  parts  $(X_1, \dots, X_N)$ , each authored by either a human or an LLM. Our goal is to segment it into human-written and LLM-generated pieces. A naïve approach is to apply a score function  $\phi$ , either a zero-shot statistical measure or

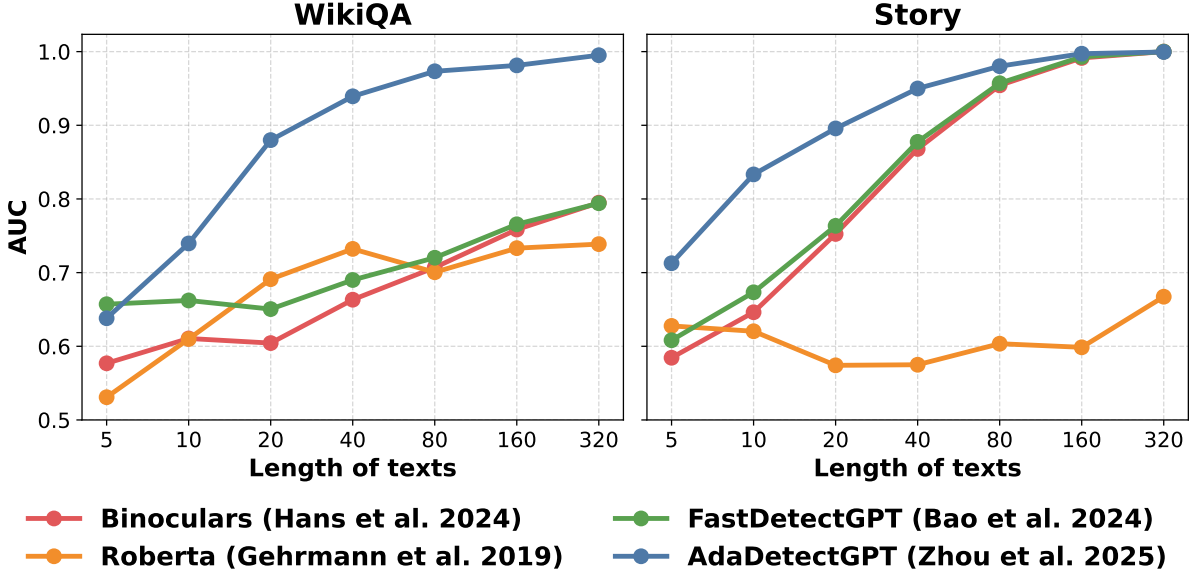


Figure 2: AUCs of various detectors on the WikiQA and Story datasets with varying lengths of input texts. RoBERTa and AdaDetectGPT are two ML-based LLM detectors, while Binoculars and FastDetectGPT are two zero-shot detectors.

an ML classifier, to assess whether each  $X_t$  is generated by an LLM. For instance,  $X_t$  is classified as LLM-authored if  $\phi(X_t)$  exceeds a certain threshold. With these classification labels at hand, we directly obtain a segmentation of the entire paragraph.

As a concrete example, each score  $\phi(X_t)$  can be set to the FastDetectGPT statistic (Bao et al., 2024). As demonstrated empirically by Bao et al. (2024), LLM-generated text typically yields higher  $\phi$  values compared to human-written text. Alternatively, we may define  $\phi(X_t)$  as the negative rewrite distance – the negative semantic distance between  $X_t$  and its LLM-rewritten version. This is motivated by the observation that LLM-generated text remains closer to its rewrite than human-authored text does (Mao et al., 2024; Yang et al., 2024).

However, such an approach suffers from two limitations: (i) The optimal classification threshold is difficult to determine a priori, and the performance of the resulting algorithm can be highly sensitive to this choice. (ii) As discussed in Section 1.1, pooling information across consecutive sentences improves detection accuracy. However, the naïve approach evaluates each sentence individually, leading to suboptimal segmentation.

To address these limitations, we frame LLM text localization as a change point detection problem. We define change points as the indices where authorship transitions between human and LLM. Formally, let  $0 = \tau_0 < \tau_1 < \dots < \tau_K < \tau_{K+1} = N$  denote  $K$  unknown change points. These points partition the paragraph into  $K + 1$  segments, such that each segment

$$X_{(\tau_i+1):\tau_{i+1}} = (X_{\tau_i+1}, X_{\tau_i+2}, \dots, X_{\tau_{i+1}})$$

is authored entirely by either a human or an LLM for every  $i \in \{0\} \cup [K]$ . Under this formulation, localizing human- or LLM-authored sentences is equivalent to identifying the set of change points  $\{\tau_k\}_{k=1}^K$  (see Figure 1 for an illustration). This enables us to leverage classical change point

detection for LLM text localization, as detailed in the next section.

Before going into the methodologies, we make a note on the initial partition  $(X_1, \dots, X_N)$  of the entire text  $X$ . In the remaining part of this work, we consider a scenario in which each  $X_t$  corresponds to a sentence. However, this is merely for convenience of description. In practice,  $X_t$  can be defined at different levels of granularity, such as paragraphs or tokens, and our framework is directly applicable in these settings as well. Generally speaking, if one uses coarse units, such as paragraphs, then the number of observations  $N$  would be small, and it is likely that a single unit already contains both human-written and LLM-authored content. If one instead uses fine units, such as treating each  $X_t$  as one token or small groups of tokens, then the sample size  $N$  and boundary resolution both increase, but neighboring scores become more dependent and the variability of the scores  $\phi(X_t)$  tends to be large due to the small segment sizes. We demonstrate the applicability of our methods in token-level segmentation in Table A2.

### 3 Methodology: From change point detection to LLM text localization

This section details our proposal for adapting change point detection to LLM-generated text localization. We begin by introducing a vanilla adaptation of the NOT algorithm (see Algorithm 1) and discussing its limitations (Section 3.1). To address these limitations, we propose a weighted algorithm (Section 3.2) and a generalized algorithm (Section 3.3). Finally, we detail the procedure for localizing human-LLM text based on the resulting change point estimates (Section 3.4).

#### 3.1 Vanilla change point detection

Having introduced the CUSUM statistic and the NOT algorithm that builds upon it, a natural approach to segmenting human-LLM co-authored text is to transform each sentence  $X_t$  in the target paragraph  $\mathbf{X}$  into a scalar  $\phi(X_t)$  using an existing detection score function  $\phi$ , such as the FastDetectGPT statistic or rewrite distance. This transformation yields a one-dimensional time series  $(\phi(X_1), \dots, \phi(X_N))$ , enabling the application of standard change point detection, such as the default NOT algorithm discussed in Section 2.2, to identify all change points  $\tau_i$ . We refer to this approach as **VCP**, short for Vanilla adaptation of Change Point detection.

However, directly applying the default NOT algorithm or other off-the-shelf change point detection algorithms is often suboptimal, as they fail to account for the heterogeneous signal strength in  $\phi(X_i)$  often resulting from varying sentence lengths<sup>1</sup>. Specifically, both theoretical results (Zhou et al., 2025) and empirical findings (Bao et al., 2024) suggest that detection accuracy increases with the length of the text. This relationship is further illustrated in Figure 2, which reports the area under the curve (AUC) for both ML-based LLM detectors and zero-shot LLM detectors across varying text lengths. The results show that detection accuracy generally increases with the input length.

---

<sup>1</sup>Even if each  $X_i$  has the same number of tokens, the variability of the detection score  $\phi(X_i)$  can be heterogeneous and may be estimated as mentioned in Section 2.1.

Consequently, change points are easier to detect when they occur near long sentences, and they become more elusive near shorter sentences. Despite this, VCP treats the level of difficulty equally across the time series, which leads to inefficient change point detection. Mathematically, this limitation stems from the use of standard CUSUM statistics in (1), which treats each observation uniformly.

Our proposed methodology, detailed in the following section, explicitly scales the contribution of each score  $\phi(X_i)$  in the CUSUM statistic according to its variability, measured by either a built-in estimate or sentence length. This scaling leads to more efficient and, in theory, *minimax optimal* segmentation for human–LLM co-authored text (see Section 4).

### 3.2 Weighted change point detection

In this section, we introduce **WCP**, a Weighted Change Point detection algorithm, to overcome the limitation of VCP. As discussed in Section 3.1, *not all sentences are created equal* for authorship identification. Rather, the difficulty of detection is inherently tied to sentence length and detection-score variability. WCP exploits this observation by assigning larger weights to more informative sentence-level detection scores and prioritizing these observations for more accurate change point detection.

Specifically, for a generic time series  $\mathbf{Y} = (Y_1, \dots, Y_N)$  and a weight vector  $w = (w_1, \dots, w_N)$ , the algorithm relies on the following weighted CUSUM statistic, defined as:

$$W_{s,e}^{\mathbf{Y}}(t) = \sqrt{\frac{S_{s:t}^w S_{(t+1):e}^w}{S_{s:e}^w}} |\bar{Y}_{s:t}^w - \bar{Y}_{(t+1):e}^w|, \quad (2)$$

where  $S_{t_1:t_2}^w = \sum_{i=t_1}^{t_2} w_i$  represents the cumulative weight, and  $\bar{Y}_{t_1:t_2}^w = (S_{t_1:t_2}^w)^{-1} \sum_{i=t_1}^{t_2} w_i Y_i$  denotes the weighted average of the observations over the interval  $[t_1, t_2]$ . By construction, a relatively larger weight  $w_i$  amplifies the impact of observation  $Y_i$  on the statistic. When  $w_i = 1$  for all  $i \in [N]$ , the weighted CUSUM is reduced to the standard CUSUM statistic in (1).

WCP applies the meta-algorithm (Algorithm 1) with  $A_{s,e}^{\mathbf{Y}}(b) = W_{s,e}^{\mathbf{Y}}(b)$  and  $B(s, e) = S_{s:e}^w$  to sentence-level scores  $(\phi(X_1), \dots, \phi(X_N))$  for change point detection. The choice of the weight vector  $w$  is critical, as it encodes sentence-specific information into the segmentation. In our theoretical analysis, we show that setting  $w_i$  to the inverse variance of each score  $\phi(X_i)$  outperforms the vanilla algorithm and achieves minimax optimal segmentation. In our implementation, we may use the variance estimator mentioned in Section 2.1 as the weights by setting  $w_i = \{\hat{\sigma}(X_i)\}^{-2}$ , or simply use sentence length as a proxy by setting  $w_i = n_i^\kappa$ , where  $n_i$  denotes the number of tokens in sentence  $X_i$  and  $\kappa > 0$  is a hyperparameter (typically set to 1 or 2).

### 3.3 Generalized change point detection

Another natural approach to enhance the performance of the vanilla algorithm is to replace the average of sentence-level scores  $\phi(X_t)$  in CUSUM with segment-level scores  $\phi(X_{t_1:t_2})$ , obtained by applying, for example, the FastDetectGPT statistic to the concatenated text  $X_{t_1:t_2}$ . This

yields the following generalized CUSUM statistic:

$$G_{s,e}^{\mathbf{X}}(t) = \sqrt{\frac{S_{s:t}^w S_{(t+1):e}^w}{S_{s:e}^w}} |\phi(X_{s:t}) - \phi(X_{(t+1):e})|. \quad (3)$$

Substituting  $A_{s,e}^{\mathbf{X}}(b)$  in Algorithm 1 with our newly defined  $G_{s,e}^{\mathbf{X}}(b)$ , and  $B(s, e)$  with  $S_{s:e}^w$ , yields the resulting algorithm, which we refer to as **GCP**, short for Generalized Change Point detection.

Compared to the standard CUSUM statistic in (1), (3) offers two advantages: (i) It aggregates information across multiple sentences, enabling the LLM detector to achieve higher classification accuracy than detecting each sentence individually. (ii) It implicitly incorporates sentence-specific attributes, such as sentence length, into the resulting score, since longer sentences likely exert a larger influence on the segment-level score. While being more general than the weighted version in (2), we show later in Theorem 4 that (3) can be equivalent to (2) under specific choices of  $\phi$ .

However, one limitation of GCP is its computational cost. In particular, implementing Algorithm 1 with the generalized CUSUM statistic requires computing the score function  $\phi$  on various segments of  $\mathbf{X}$ , due to the recursive nature of the algorithm. In contrast, VCP and WCP only require a single pass of  $\phi$  over each individual sentence  $X_i$ .

### 3.4 Human-LLM text localization

After obtaining the estimated change points  $\hat{\tau}_1 < \dots < \hat{\tau}_{\hat{K}}$ , we divide the whole passage into  $\hat{K} + 1$  segments

$$X_{1:\hat{\tau}_1}, X_{\hat{\tau}_1+1:\hat{\tau}_2}, \dots, X_{(\hat{\tau}_{\hat{K}-1}+1):\hat{\tau}_{\hat{K}}}, X_{(\hat{\tau}_{\hat{K}}+1):N},$$

where  $\hat{K}$  denotes our estimated number of change points. We next apply  $\phi$  to these segments to calculate their detection scores  $\{\phi(X_{1:\hat{\tau}_1}), \phi(X_{\hat{\tau}_1+1:\hat{\tau}_2}), \dots, \phi(X_{(\hat{\tau}_{\hat{K}}+1):N})\}$ , and employ a clustering algorithm (e.g.,  $k$ -means with  $k = 2$ ) to group these segment-wise scores into two clusters. Given our construction of  $\phi$  where higher values indicate a larger probability of LLM generation, the cluster with the larger mean is classified as LLM-authored, while the other cluster is identified as human-authored.

## 4 Theory

**Summary.** In this section, we develop theoretical guarantees for the proposed algorithms in Section 3. We begin with a summary of our main findings:

- **Non-asymptotic error bound:** Theorems 1 and 2 establish non-asymptotic bounds on the localization error (i.e., distance between the estimated change points and their oracle locations) for VCP and WCP, respectively. Crucially, VCP’s error bound is governed by the maximal variance of the sentence-level scores, whereas the bound for WCP depends on their harmonic mean. Since the harmonic mean is strictly bounded by the maximum, these results formally demonstrate that WCP outperforms VCP, particularly in the presence of heterogeneous variances. In the homogeneous case, the two algorithms achieve equivalent performance.

- **Minimax optimality:** Theorem 3 derives a minimax lower bound for the change point estimation error. Notably, this lower bound matches the upper bound achieved by WCP. Together with Theorem 2, this establishes the *minimax optimality of WCP*. Furthermore, we show the equivalence of WCP and GCP under appropriate conditions in Theorem 4, which effectively extends *minimax optimality to GCP*. To the best of our knowledge, minimax rates of this form with delicate dependence on the heterogeneous variance parameters have not been established, even in the change point literature.

**Non-asymptotic error bound.** We next detail these results. Suppose there are  $K$  change points  $\{\tau_j\}_{j \in [K]}$  in a paragraph  $\mathbf{X} = (X_1, \dots, X_N)$ . Let  $\Delta_1 = \min_{j \in [K+1]} \{\tau_j - \tau_{j-1}\}$  denote the minimum gap between these change points. Furthermore, let  $\mu_h = \mathbb{E}[\phi(X_h)]$  and  $\mu_m = \mathbb{E}[\phi(X_m)]$  denote the expected scores for a human-authored sentence  $X_h$  and an LLM-authored sentence  $X_m$ , respectively. Let  $\sigma_i$  denote the sub-Gaussian parameter of  $\phi(X_i)$ , defined in (9); we simply refer to  $\sigma_i^2$  as the variance proxy of  $\phi(X_i)$  in the main text. The following theorem upper bounds the localization error of VCP (Section 3.1).

**Theorem 1** (Error bound for VCP). *Under the assumptions and appropriate choice of tuning parameters specified in Appendix A.1, if there exist some absolute constant  $c > 0$  and some  $0 < \delta < 1$  such that*

$$(\mu_m - \mu_h)^2 \Delta_1 \geq c \sigma_{\max}^2 \log(N/\delta), \quad (4)$$

where  $\sigma_{\max}^2 = \max_{i \in [N]} \sigma_i^2$ , then with probability at least  $1 - \delta$ , the outputs of VCP  $\{\hat{\tau}_j\}_{j \in [\hat{K}]}$  and  $\hat{K}$  satisfy that

$$\hat{K} = K \text{ and } \max_{j \in [K]} |\hat{\tau}_j - \tau_j| = O\left(\frac{\sigma_{\max}^2 \log(N/\delta)}{(\mu_m - \mu_h)^2}\right). \quad (5)$$

Theorem 1 shows that with high probability, VCP recovers the true number of change points and upper bounds the localization error as specified in (5). However, the upper bound depends on the maximal variance  $\sigma_{\max}^2$ , which is quite pessimistic. In practice, if even a single score  $\phi(X_i)$  exhibits high variance – often the case for short sentences with limited tokens – the resulting bound becomes considerably large. This suggests that VCP’s theoretical performance is limited by the least reliable sentence classification in the paragraph.

The condition in (4) is called the signal-to-noise ratio (SNR) condition, which requires that the detectable signal, represented by the left-hand side (LHS) of (4), dominates the noise level on the right-hand side (RHS). The signal strength in this context is a product of two components: (a)  $(\mu_m - \mu_h)^2$ , which measures how well  $\phi$  can distinguish human- and LLM-authored text, and (b)  $\Delta_1$ , the minimal distance between two consecutive change points. Notably, the RHS is also scaled by  $\sigma_{\max}^2$ , which can be quite restrictive in practice.

We next demonstrate how WCP (Section 3.2) improves both the signal-to-noise condition (4) and the error bound (5) in the following theorem.

**Theorem 2** (Error bound for WCP). *Under the same assumptions specified in Appendix A.1, together with the signal-to-noise condition in (4), if we choose  $w_i = \sigma_i^{-2}$  and  $B(s, e) = e - s$  in*

the WCP algorithm, its outputs,  $\{\hat{\tau}_j\}_{j \in [\hat{K}]}$  and  $\hat{K}$  satisfy that, with probability at least  $1 - \delta$ ,

$$\hat{K} = K \text{ and } \sum_{i \in (\tau_j, \hat{\tau}_j] \cup (\hat{\tau}_j, \tau_j]} \frac{1}{\sigma_i^2} = O\left(\frac{\log(N/\delta)}{(\mu_m - \mu_h)^2}\right), \forall j. \quad (6)$$

Moreover, let  $\Delta_2 = \min_{j \in [K+1]} \sum_{i=\tau_{j-1}+1}^{\tau_j} \sigma_i^{-2}$ . If  $\max_{i \in [N]} \sigma_i^{-2} = O(\Delta_2)$ ,  $M \geq N^2 \log(K/\delta)$  and  $B(s, e) = S_{s:e}^w$ , then the SNR condition in (4) can be replaced by

$$(\mu_m - \mu_h)^2 \Delta_2 \geq c \log(N/\delta), \quad (7)$$

for some absolute constant  $c > 0$ , while the result in (6) still holds.

The error bound in (6) measures the weighted distance between the estimated and true change points. To provide intuition, consider the case where the variance  $\sigma_i^2$  is inversely proportional to the sentence length  $n_i$  (i.e.,  $\sigma_i^2 \propto n_i^{-1}$ ). In this scenario, the term  $\sum \sigma_i^{-2}$  in (6) represents the total number of tokens between  $\tau_j$  and  $\hat{\tau}_j$ .

Comparing Theorem 1 with Theorem 2, we see that WCP outperforms VCP in two aspects. First, under the same SNR condition (4), WCP achieves a smaller localization error. This is because

$$\frac{|\tau_j - \hat{\tau}_j|}{\sigma_{\max}^2} \leq \sum_{i \in (\tau_j, \hat{\tau}_j] \cup (\hat{\tau}_j, \tau_j]} \frac{1}{\sigma_i^2},$$

and hence (6) implies (5). Second, WCP obtains the stronger guarantee even under a weaker SNR condition (7), allowing more subtle changes in the signal to be detected. Specifically, the requirement in (7) is less stringent than that of (4) because

$$\Delta_2 = \min_{j \in [K+1]} \sum_{i=\tau_{j-1}+1}^{\tau_j} \frac{1}{\sigma_i^2} \geq \frac{\Delta_1}{\sigma_{\max}^2},$$

which offers a stronger signal on the left-hand side. The proof of (6) under the weaker condition (7) relies on refined theoretical arguments at the ‘‘token’’ level, instead of the ‘‘sentence’’ level.

**Minimax optimality.** We next show that the localization error achieved by WCP is minimax optimal. To present the minimax lower bound, we introduce the following notation. For a given  $\delta \in (0, 1/2)$ , an estimator  $\hat{\tau}$  and a distribution  $P$ , let

$$Q(\delta, \hat{\tau}, P) := \inf\{\eta \in [0, \infty) : P(|\hat{\tau} - \tau| \leq \eta) \geq 1 - \delta\},$$

which can be interpreted as the smallest localisation error that can be achieved by  $\hat{\tau}$  with probability at least  $1 - \delta$ .

**Theorem 3** (Minimax lower bound). *Suppose Assumptions (i) and (ii) in Appendix A.1 hold. Suppose that there is only one change point  $1 < \tau < N$  representing a transition from LLM-authored to human-authored text. Let  $P$  denote the joint distribution of  $\{\phi(X_i)\}_{i \in [N]}$ . Consider*

the class of distributions

$$\mathcal{P} = \left\{ P : (\mu_m - \mu_h)^2 \min\{S_{1:\tau}^w, S_{(\tau+1):N}^w\} \geq C \log(1/\delta) \right\},$$

with  $w_i = \sigma_i^{-2}$ , for some absolute constant  $C > 0$ . It holds that

$$\inf_{\hat{\tau}} \sup_{P \in \mathcal{P}} Q(\delta, \hat{\tau}, P) \geq \max\{h_1, h_2\},$$

where  $h_1$  and  $h_2$  satisfy

$$\sum_{\tau+1}^{\tau+h_1} \frac{1}{\sigma_i^2} = \frac{c \log(1/\delta)}{(\mu_m - \mu_h)^2}, \quad \sum_{\tau-h_2}^{\tau} \frac{1}{\sigma_i^2} = \frac{c \log(1/\delta)}{(\mu_m - \mu_h)^2}, \quad (8)$$

for some constant  $c > 0$ .

To see that the guarantee in Theorem 2 is minimax optimal, we set the failure probability  $\delta = N^{-1}$ , which is a natural choice to ensure that (6) holds with probability approaching 1 as  $N \rightarrow \infty$ . Without loss of generality, we consider the upper bound in the case of a single change point. When  $\hat{\tau} > \tau$ , (6) becomes

$$\sum_{\tau+1}^{\hat{\tau}} \frac{1}{\sigma_i^2} = O\left(\frac{\log(N)}{(\mu_m - \mu_h)^2}\right),$$

which together with the definition of  $h_1$  in (8), immediately implies  $\hat{\tau} - \tau = O(h_1)$ . Similarly, we have  $\tau - \hat{\tau} = O(h_2)$  when  $\tau > \hat{\tau}$ . Combining these two cases, we conclude that WCP's estimated change point satisfies

$$|\hat{\tau} - \tau| = O(\max\{h_1, h_2\}),$$

and therefore matches the lower bound up to constants in Theorem 3.

To conclude this section, the following informal theorem establishes the equivalence between WCP and GCP, so that the minimax optimality applies to GCP as well. See Appendix A.3 for the full statement.

**Theorem 4** (Equivalence). *Suppose  $\phi$  is set to either a zero-shot detection statistic or an ML-based detection statistic evaluating a rewrite distance. Under appropriate conditions, the generalized CUSUM statistic (3) equals the weighted CUSUM statistic (2), i.e.  $G_{s,e}^{\mathbf{X}}(t) = W_{s,e}^{\mathbf{Y}}(t)$  for all  $t \in [N]$ , with  $Y = (\phi(X_1), \dots, \phi(X_N))$ , and therefore WCP is equivalent to GCP.*

## 5 Experiments

This section presents extensive experiments to assess the empirical performance of our approach. In Section 5.1, we first study the setting with a single change point, and then extend the evaluation to multiple change points in Section 5.2. Section 5.3 further conducts a sensitivity analysis under more complicated data-generating settings that may affect the performance of our method. We conclude the section with a real-world study involving manually manipulated

text (see Section 5.4).

Below, we first describe the basic setup in simulation. More experimental details are provided in Appendix C.

- **Datasets.** We first describe our procedure for generating human–LLM co-authored text. We randomly sample 100 documents from each of three publicly available datasets: *WikiQA* (Rajpurkar et al., 2016), *News* (Narayan et al., 2018), and *Story* (Fan et al., 2018). For each document, we split the text into multiple segments. We then prompt LLMs to regenerate some segments while keeping the remaining segments in their original human-authored form. To ensure diversity, several models are employed, including GPT-5-mini (Singh et al., 2025) and Claude 4.5 (Anthropic, 2025). Details regarding the specific prompts used for LLM rewriting are provided in Appendix C.
- **Evaluation metric.** We use the WindowDiff (WD) metric proposed by Pevzner & Hearst (2002). Its definition is provided in Appendix C. We also add count error (CE), which denotes the difference between the true number of change points and the estimated number. A negative CE indicates overestimation of the number of change points. We report the average WD and CE across 100 documents for every combination of LLM generator and dataset.
- **Methods.** We compare VCP, WCP, a sentence-level prediction baseline (denoted by SenPred, Kushnareva et al., 2024), a majority-voting algorithm (denoted by Voting, Zhang et al., 2024b), direct prompting of the LLM that rewrites the paragraph to segment the human–LLM co-authored text (denoted by LLMPred), TextTiling (Hearst, 1997), and a partial LLM detector (PaLD, Lei et al., 2025).

To ensure fairness among score-based methods, we use the same detection score,  $\phi$ , for segmentation. We consider several choices of  $\phi$ : an ML-based score from AdaDetectGPT (Zhou et al., 2025), and zero-shot scores derived from FastDetectGPT and log likelihood (Gehrmann et al., 2019; Bao et al., 2024). The main text presents results obtained using AdaDetectGPT.

## 5.1 Single change point detection

We first evaluate whether the proposed change-point formulation can localize a single transition between human-written and LLM-written text. When generating the co-authored text, the change-point location is sampled at random for each document. This setting better reflects practical cases, where the LLM-written segment may appear at an arbitrary position. Table 1 reports the results under this single random change-point setting.

Table 1: Results on single change-point detection. The best results are presented in **bold**. PaLD is associated with high computational cost; thus, its results on the News and Story datasets are omitted.

Model	Method	WikiQA		News		Story	
		WD	CE	WD	CE	WD	CE
Claude 4.5	TextTiling	0.422	-0.475	1.176	-4.560	0.805	-2.970
	LLMPred	0.588	-0.859	1.155	-3.360	1.526	-4.620
	SenPred	0.388	-1.374	1.739	-6.970	2.343	-9.430
	Voting	0.308	-0.192	0.184	-0.620	0.443	-1.480
	PaLD	0.489	-1.525	–	–	–	–
	VCP	0.231	<b>-0.010</b>	0.191	<b>0.000</b>	0.272	<b>0.000</b>
	WCP	<b>0.227</b>	<b>-0.010</b>	<b>0.120</b>	<b>0.000</b>	<b>0.207</b>	<b>0.000</b>
GPT-5-mini	TextTiling	0.418	-0.465	1.324	-5.120	0.969	-3.480
	LLMPred	0.477	-0.606	1.206	-3.630	1.361	-4.020
	SenPred	0.636	-2.030	2.769	-11.430	2.859	-11.460
	Voting	0.372	-0.465	0.863	-3.150	0.925	-3.370
	PaLD	0.685	-2.202	–	–	–	–
	VCP	0.363	<b>-0.010</b>	0.369	<b>0.000</b>	0.356	<b>0.000</b>
	WCP	<b>0.345</b>	<b>-0.010</b>	<b>0.314</b>	<b>0.000</b>	<b>0.321</b>	<b>0.000</b>

Table 1 leads to the following observations.

1. WCP attains the smallest WD across all six model–dataset combinations. The improvement is particularly clear on the News and Story datasets, where sentence-wise prediction and direct LLM prompting produce substantially larger segmentation errors.
2. VCP also controls the number of detected change points, with CE essentially matching that of WCP. However, its WD is consistently larger than that of WCP, which is consistent with the theoretical role of weighting in improving localization under heterogeneous sentence-level detection noise.
3. The baseline methods often have negative CE, indicating a tendency to over-detect changes, and this over-detection is accompanied by larger WD. One reason is that their objectives are not fully aligned with the human–LLM boundary localization problem. TextTiling segments text by semantic coherence, whereas semantic shifts need not coincide with provenance shifts between human-written and LLM-written segments. Voting, SenPred, and LLMPred make sentence- or window-level decisions without explicitly enforcing a change-point structure. These results support the main mechanism of our approach: imposing a change-point structure on sentence-level detection scores improves boundary localization in mixed human–LLM documents.
4. PaLD is closer in spirit to our objective, but its greedy search may lead to suboptimal segmentation. This comparison suggests that the change-point detection procedure used to

select segment boundaries plays an important role in reliable localization.

## 5.2 Results on multiple change points

In this part, we consider settings with multiple change points where the number of change points  $K$  varies within  $\{1, 2, 3, 5, 8\}$ . For each document, we evenly split the text into  $K + 1$  segments, each containing approximately the same number of sentences. The 1st, 3rd, 5th,  $\dots$  segments are unchanged, while the remaining segments are written by an LLM. PaLD is not included in this or subsequent experiments due to its computational cost.

Table 2: Results on multiple change-point detection on the Story dataset. The best results are presented in **bold**.

Model	Method	$K = 1$		$K = 2$		$K = 3$		$K = 5$		$K = 8$	
		WD	CE	WD	CE	WD	CE	WD	CE	WD	CE
Claude 4.5	TextTiling	0.75	-2.68	0.77	-3.80	0.72	-4.47	0.64	-4.64	0.53	-3.06
	LLMPred	1.42	-4.24	1.23	-4.68	1.05	-4.43	0.52	2.27	0.49	4.96
	SenPred	2.18	-8.70	2.24	-13.80	2.19	-17.91	1.89	-23.38	1.31	-24.68
	Voting	0.38	-1.23	0.45	-2.19	0.46	-2.78	0.38	-2.71	<b>0.33</b>	-2.56
	VCP	0.31	-1.73	0.33	-2.81	<b>0.31</b>	-2.90	<b>0.32</b>	-3.35	<b>0.33</b>	-1.22
	WCP	<b>0.26</b>	<b>-1.11</b>	<b>0.29</b>	<b>-1.01</b>	<b>0.31</b>	<b>-1.13</b>	0.33	<b>-0.91</b>	<b>0.33</b>	<b>0.68</b>
GPT-5-mini	TextTiling	0.96	-3.47	1.05	-5.34	0.91	-6.10	0.75	-6.50	0.61	-5.20
	LLMPred	1.34	-4.02	1.20	-4.74	1.12	-5.06	0.56	1.45	0.51	4.46
	SenPred	2.68	-10.94	2.89	-17.90	2.92	-24.38	2.42	-30.43	1.79	-33.54
	Voting	0.40	-0.50	0.47	-0.28	0.46	0.86	0.82	-7.60	0.65	-6.39
	VCP	0.41	<b>-0.47</b>	0.50	-1.64	0.51	-2.01	0.51	-1.52	0.46	<b>0.65</b>
	WCP	<b>0.39</b>	-0.88	<b>0.41</b>	<b>0.05</b>	<b>0.43</b>	<b>0.24</b>	<b>0.44</b>	<b>0.76</b>	<b>0.43</b>	1.91

Table 2 shows that WCP remains competitive as the number of change points increases. Across both LLM generators, WCP achieves the best or near-best WD in most settings. VCP also performs strongly because it uses the same change-point structure, but its larger WD in many settings indicates that unweighted segmentation is less powerful when sentence-level detection scores are heterogeneous. In contrast, the baseline methods often incur larger WD or CE, which is consistent with the single-change-point results.

## 5.3 Sensitivity analysis

We further study two data-generation factors that may affect localization performance: adversarial attacks on the text and the proportion of LLM-written content.

**Adversarial attack.** We consider two adversarial settings: (1) decoherence and (2) paraphrasing. For decoherence, we perturb LLM-generated sentences to reduce their coherence, making

them closer to human-written text that may not be perfectly coherent. Specifically, we use a lightweight attack that randomly swaps one adjacent word pair within each LLM-generated sentence. For paraphrasing, we perturb human-written sentences by using a language model to rephrase them, making them closer to LLM-generated text. Results under the two attacks are presented in Table 3.

Although these perturbations increase the difficulty of localization, WCP generally achieves the best performance across the two adversarial settings. Its WD also increases more mildly than those of the baselines, suggesting that the change-point formulation remains useful when sentence-level detection signals are weakened.

Table 3: Results on two adversarial attack setups.

Setup	Method	WikiQA		News		Story	
		WD	CE	WD	CE	WD	CE
decoherence	TextTiling	0.418	-0.465	1.320	-5.110	0.969	-3.480
	LLMPred	0.490	-0.687	1.193	-3.740	1.217	-3.450
	SenPred	0.696	-2.172	2.941	-12.150	2.892	-11.800
	Voting	0.441	-0.657	0.950	-3.480	0.929	-3.390
	WCP	<b>0.370</b>	<b>-0.010</b>	<b>0.380</b>	<b>0.000</b>	<b>0.354</b>	<b>0.000</b>
paraphrase	TextTiling	0.417	-0.485	1.313	-5.130	0.957	-3.430
	LLMPred	0.540	-0.949	0.879	-2.230	1.216	-3.500
	SenPred	0.675	-2.162	2.858	-11.800	3.076	-12.580
	Voting	<b>0.400</b>	-0.455	0.944	-3.450	1.018	-3.910
	WCP	0.412	<b>-0.010</b>	<b>0.421</b>	<b>0.000</b>	<b>0.379</b>	<b>0.000</b>

**Varying proportion of LLM-written content.** We next use the Story dataset to study how performance changes with the proportion of LLM-written content. For each document, we keep an initial proportion of sentences as human-written and generate the remaining sentences using an LLM. We vary this proportion within {5%, 10%, 20%, 40%, 80%}. Table 4 shows the results of WCP and baselines. WCP consistently achieves smaller WD and more stable CE across different LLM-authored proportions, indicating that the proposed localization procedure remains effective when the relative lengths of human-written and LLM-written segments vary.

Table 4: Performance of various methods on different proportions of LLM-written content on the Story dataset.

Method	5%		10%		20%		40%		80%	
	WD	CE	WD	CE	WD	CE	WD	CE	WD	CE
TextTiling	0.97	-7.77	0.97	-7.77	0.94	-7.62	0.93	-6.98	0.92	-5.58
LLMPred	0.93	-8.72	0.94	-8.59	0.90	-8.04	0.86	-7.89	0.91	-8.20
SenPred	1.00	-37.44	1.00	-36.80	0.99	-35.73	0.99	-36.46	1.00	-37.16
Voting	0.69	-8.90	0.48	-5.40	0.46	-5.12	0.52	-6.58	0.81	-11.19
WCP	<b>0.26</b>	<b>-2.84</b>	<b>0.21</b>	<b>-2.99</b>	<b>0.24</b>	<b>-2.80</b>	<b>0.29</b>	<b>-2.65</b>	<b>0.44</b>	<b>-2.71</b>

#### 5.4 The CoAuthor Dataset Analysis

We next evaluate our method on the human–AI co-authored text dataset provided by [Lee et al. \(2022\)](#). The CoAuthor data were collected through a custom text-editor interface. At the beginning of each session, writers were given a prompt and asked to write either a creative story or an argumentative essay. During writing, they could request GPT-3 suggestions through a shortcut whenever needed. The interface logged the full interaction trace, including writers’ own text, GPT-3 suggestions, whether suggestions were accepted or dismissed, and subsequent edits to accepted suggestions or previous text. In total, CoAuthor contains 1,445 writing sessions produced by 63 writers interacting with four GPT-3 instances, including 830 creative-writing stories and 615 argumentative-writing essays.

Following the setup in [Zeng et al. \(2024a\)](#), each document is annotated at the sentence level with three labels: human-written, collaboratively written, and fully LLM-generated sentences. This setting turns localization into a three-class segmentation problem, which is more challenging than the binary human–LLM setting and better reflects practical human–AI co-authoring scenarios. We also compare a strong supervised baseline considered in [Zeng et al. \(2024a\)](#), SegFormer ([Bai et al., 2023](#)). Since pretrained checkpoints for SegFormer are not publicly available, we train the model from scratch. We split the CoAuthor dataset into training (60%), validation (20%), and test (20%) sets, and report all results on the held-out test set. We also include the baseline methods considered in the preceding experiments. Because the task has three classes, we apply the clustering procedure in Section 3.4 to assign detection scores to the three labels.

The results on the CoAuthor dataset are summarized in Table 5. VCP and WCP achieve the smallest WD, indicating better boundary localization on this real-world co-authoring dataset. SegFormer obtains the smallest absolute CE, which is expected for a supervised model trained on the dataset, but its WD remains larger than that of the proposed change-point methods. Unsupervised baselines, such as Voting and TextTiling, have substantially larger WD, suggesting that they remain less effective at handling segmentation tasks in this three-class setting.

Table 5: Results on the real-world CoAuthor dataset.

	WD	CE
TextTiling	0.66	-6.76
LLMPred	0.64	-6.25
SenPred	0.70	-11.68
Voting	0.51	-2.65
SegFormer	0.39	<b>2.45</b>
VCP	<b>0.36</b>	2.63
WCP	<b>0.36</b>	2.71

## 6 Conclusion

This paper proposes a change point detection approach to localize human- and LLM-authored text in hybrid human–LLM documents. We develop three algorithms to address this largely unexplored problem, establish their finite-sample error guarantees and minimax optimality, and demonstrate their superior empirical performance. By bridging the change point detection literature with modern LLMs, our work paves the way for leveraging classical time-series tools to solve the evolving challenges posed by LLM-generated content.

## References

- Anthropic. System card:claude sonnet 4.5. 2025. URL <https://www-cdn.anthropic.com/963373e433e489a87a10c823c52a0a013e9172dd.pdf>.
- Bai, H., Wang, P., Zhang, R., and Su, Z. Segformer: a topic segmentation model with controllable range of attention. In *Proceedings of the AAAI conference on artificial intelligence*, volume 37, pp. 12545–12552, 2023.
- Bao, G., Zhao, Y., Teng, Z., Yang, L., and Zhang, Y. Fast-DetectGPT: Efficient zero-shot detection of machine-generated text via conditional probability curvature. In *The Twelfth International Conference on Learning Representations*, 2024.
- Baranowski, R., Chen, Y., and Fryzlewicz, P. Narrowest-over-threshold detection of multiple change points and change-point-like features. *Journal of the Royal Statistical Society Series B: Statistical Methodology*, 81(3):649–672, 2019.
- Bhattacharyya, S. and Ramdas, A. Theoretical guarantees for change localization using conformal p-values. *arXiv preprint arXiv:2510.08749*, 2025.
- Bird, S., Klein, E., and Loper, E. *Natural language processing with Python: analyzing text with the natural language toolkit*. " O'Reilly Media, Inc.", 2009.
- Chen, J., Zhu, X., Liu, T., Chen, Y., Xinhui, C., Yuan, Y., Leong, C. T., Li, Z., Tang, L., Zhang, L., et al. Imitate before detect: Aligning machine stylistic preference for machine-revised text

- detection. In *Proceedings of the AAAI Conference on Artificial Intelligence*, volume 39, pp. 23559–23567, 2025.
- Cho, H. and Kirch, C. Two-stage data segmentation permitting multiscale change points, heavy tails and dependence. *Annals of the Institute of Statistical Mathematics*, 74(4):653–684, 2022.
- Comanici, G., Bieber, E., Schaeckermann, M., Pasupat, I., Sachdeva, N., Dhillon, I., Blistein, M., Ram, O., Zhang, D., Rosen, E., et al. Gemini 2.5: Pushing the frontier with advanced reasoning, multimodality, long context, and next generation agentic capabilities. *arXiv preprint arXiv:2507.06261*, 2025.
- Dugan, L., Ippolito, D., Kirubarajan, A., Shi, S., and Callison-Burch, C. Real or fake text? investigating human ability to detect boundaries between human-written and machine-generated text. In *Proceedings of the Thirty-Seventh AAAI Conference on Artificial Intelligence and Thirty-Fifth Conference on Innovative Applications of Artificial Intelligence and Thirteenth Symposium on Educational Advances in Artificial Intelligence*, AAAI’23/IAAI’23/EAAI’23. AAAI Press, 2023.
- Fan, A., Lewis, M., and Dauphin, Y. Hierarchical neural story generation. In Gurevych, I. and Miyao, Y. (eds.), *Proceedings of the 56th Annual Meeting of the Association for Computational Linguistics (Volume 1: Long Papers)*, pp. 889–898, Melbourne, Australia, July 2018. Association for Computational Linguistics.
- Fryzlewicz, P. Wild binary segmentation for multiple change-point detection. *The Annals of Statistics*, 42(6):2243–2281, 2014. doi: 10.1214/14-AOS1245.
- Gehrmann, S., Strobelt, H., and Rush, A. GLTR: Statistical detection and visualization of generated text. In Costa-jussà, M. R. and Alfonseca, E. (eds.), *Proceedings of the 57th Annual Meeting of the Association for Computational Linguistics: System Demonstrations*, pp. 111–116, Florence, Italy, July 2019. Association for Computational Linguistics.
- Guo, B., Zhang, X., Wang, Z., Jiang, M., Nie, J., Ding, Y., Yue, J., and Wu, Y. How close is ChatGPT to human experts? comparison corpus, evaluation, and detection. *arXiv preprint arXiv:2301.07597*, 2023.
- Guo, H., Cheng, S., Jin, X., Zhang, Z., Zhang, K., Tao, G., Shen, G., and Zhang, X. Biscope: AI-generated text detection by checking memorization of preceding tokens. *Advances in Neural Information Processing Systems*, 37:104065–104090, 2024.
- Hans, A., Schwarzschild, A., Cherepanova, V., Kazemi, H., Saha, A., Goldblum, M., Geiping, J., and Goldstein, T. Spotting LLMs with binoculars: zero-shot detection of machine-generated text. In *Proceedings of the 41st International Conference on Machine Learning*, 2024.
- Hearst, M. A. Text tiling: Segmenting text into multi-paragraph subtopic passages. *Computational linguistics*, 23(1):33–64, 1997.
- Hu, X., Chen, P.-Y., and Ho, T.-Y. Radar: Robust AI-text detection via adversarial learning. *Advances in neural information processing systems*, 36:15077–15095, 2023.

- Ippolito, D., Duckworth, D., Callison-Burch, C., and Eck, D. Automatic detection of generated text is easiest when humans are fooled. In Jurafsky, D., Chai, J., Schluter, N., and Tetreault, J. (eds.), *Proceedings of the 58th Annual Meeting of the Association for Computational Linguistics*, pp. 1808–1822, Online, July 2020. Association for Computational Linguistics.
- Jiang, L., Wu, D., and Zheng, X. SenDetEX: Sentence-level AI-generated text detection for human-AI hybrid content via style and context fusion. In Christodoulopoulos, C., Chakraborty, T., Rose, C., and Peng, V. (eds.), *Proceedings of the 2025 Conference on Empirical Methods in Natural Language Processing*, pp. 5287–5302, Suzhou, China, November 2025. Association for Computational Linguistics. ISBN 979-8-89176-332-6.
- Kushnareva, L., Gaintseva, T., Magai, G., Barannikov, S., Abulkhanov, D., Kuznetsov, K., Tulchinskii, E., Piontkovskaya, I., and Nikolenko, S. Ai-generated text boundary detection with roft. In *First Conference on Language Modeling*, 2024.
- Lee, M., Liang, P., and Yang, Q. Coauthor: Designing a human-ai collaborative writing dataset for exploring language model capabilities. In *Proceedings of the 2022 CHI conference on human factors in computing systems*, pp. 1–19, 2022.
- Lei, E., Hsu, H., and Chen, C.-F. Pald: Detection of text partially written by large language models. In *The Thirteenth International Conference on Learning Representations*, 2025.
- Li, M. and Yu, Y. Adversarially robust change point detection. *Advances in Neural Information Processing Systems*, 34:22955–22967, 2021.
- Li, M., Berrett, T., and Yu, Y. Network change point localisation under local differential privacy. *Advances in Neural Information Processing Systems*, 35:15013–15026, 2022.
- Li, X., Li, G., and Zhang, X. Segmenting watermarked texts from language models. *Advances in Neural Information Processing Systems*, 37:14634–14665, 2024.
- Liu, H., Gao, C., and Samworth, R. J. Minimax rates in sparse, high-dimensional changepoint detection. *The Annals of Statistics*, 49(2):1081–1112, 2021. doi: 10.1214/20-AOS1994.
- Ma, T., Verchand, K. A., and Samworth, R. J. High-probability minimax lower bounds. *arXiv preprint arXiv:2406.13447*, 2024.
- Madrid Padilla, C. M., Xu, H., Wang, D., MADRID PADILLA, O. H., and Yu, Y. Change point detection and inference in multivariate non-parametric models under mixing conditions. *Advances in Neural Information Processing Systems*, 36:21081–21134, 2023.
- Mao, C., Vondrick, C., Wang, H., and Yang, J. Raidar: generative AI detection via rewriting. In *The Twelfth International Conference on Learning Representations*, 2024.
- Mitchell, E., Lee, Y., Khazatsky, A., Manning, C. D., and Finn, C. Detectgpt: Zero-shot machine-generated text detection using probability curvature. In *International Conference on Machine Learning*, pp. 24950–24962. PMLR, 2023.
- Narayan, S., Cohen, S. B., and Lapata, M. Don’t give me the details, just the summary!

- topic-aware convolutional neural networks for extreme summarization. *ArXiv*, abs/1808.08745, 2018.
- OpenAI. GPT-5 system card. 2025. URL <https://cdn.openai.com/gpt-5-system-card.pdf>.
- Padilla, O. H. M., Yu, Y., Wang, D., and Rinaldo, A. Optimal nonparametric multivariate change point detection and localization. *IEEE Transactions on Information Theory*, 68(3): 1922–1944, 2021.
- Pevzner, L. and Hearst, M. A. A critique and improvement of an evaluation metric for text segmentation. *Computational Linguistics*, 28(1):19–36, 2002.
- Rajpurkar, P., Zhang, J., Lopyrev, K., and Liang, P. SQuAD: 100,000+ questions for machine comprehension of text. In Su, J., Duh, K., and Carreras, X. (eds.), *Proceedings of the 2016 Conference on Empirical Methods in Natural Language Processing*, pp. 2383–2392, Austin, Texas, November 2016. Association for Computational Linguistics.
- Singh, A., Fry, A., Perelman, A., Tart, A., Ganesh, A., El-Kishky, A., McLaughlin, A., Low, A., Ostrow, A., Ananthram, A., et al. Openai gpt-5 system card. *arXiv preprint arXiv:2601.03267*, 2025.
- Solaiman, I., Brundage, M., Clark, J., Askill, A., Herbert-Voss, A., Wu, J., Radford, A., Krueger, G., Kim, J. W., Kreps, S., et al. Release strategies and the social impacts of language models. *arXiv preprint arXiv:1908.09203*, 2019.
- Song, Y., Yuan, Z., Zhang, S., Fang, Z., Yu, J., and Liu, F. Deep kernel relative test for machine-generated text detection. In *The Thirteenth International Conference on Learning Representations*, 2025.
- Su, J., Zhuo, T., Wang, D., and Nakov, P. DetectLLM: Leveraging log rank information for zero-shot detection of machine-generated text. In Bouamor, H., Pino, J., and Bali, K. (eds.), *Findings of the Association for Computational Linguistics: EMNLP 2023*, pp. 12395–12412, Singapore, December 2023. Association for Computational Linguistics.
- Su, Z., Wang, Y., Wan, H., Zhang, Z., and Luo, M. HACo-det: A study towards fine-grained machine-generated text detection under human-AI coauthoring. In Che, W., Nabende, J., Shutova, E., and Pilehvar, M. T. (eds.), *Proceedings of the 63rd Annual Meeting of the Association for Computational Linguistics (Volume 1: Long Papers)*, pp. 22015–22036, Vienna, Austria, July 2025. Association for Computational Linguistics.
- Tian, Y., Chen, H., Wang, X., Bai, Z., ZHANG, Q., Li, R., Xu, C., and Wang, Y. Multiscale positive-unlabeled detection of AI-generated texts. In *The Twelfth International Conference on Learning Representations*, 2024.
- Tulchinskii, E., Kuznetsov, K., Kushnareva, L., Cherniavskii, D., Nikolenko, S., Burnaev, E., Barannikov, S., and Piontkovskaya, I. Intrinsic dimension estimation for robust detection of AI-generated texts. In *Advances in Neural Information Processing Systems*, volume 36, pp. 39257–39276, 2023.

- Vershynin, R. *High-dimensional probability: An introduction with applications in data science*, volume 47. Cambridge university press, 2018.
- Verzelen, N., Fromont, M., Lerasle, M., and Reynaud-Bouret, P. Optimal change-point detection and localization. *The Annals of Statistics*, 51(4):1586–1610, 2023.
- Wang, D., Yu, Y., and Rinaldo, A. Univariate mean change point detection: Penalization, cusum and optimality. *Electronic Journal of Statistics*, 14(1):1917–1961, 2020. doi: 10.1214/20-EJS1710.
- Wang, D., Yu, Y., and Rinaldo, A. Optimal change point detection and localization in sparse dynamic networks. *The Annals of Statistics*, 49(1):203–232, 2021.
- Wang, P., Li, L., Ren, K., Jiang, B., Zhang, D., and Qiu, X. SeqXGPT: Sentence-level AI-generated text detection. In Bouamor, H., Pino, J., and Bali, K. (eds.), *Proceedings of the 2023 Conference on Empirical Methods in Natural Language Processing*, pp. 1144–1156, Singapore, December 2023. Association for Computational Linguistics.
- xAI. Grok 4 model card. 2025. URL <https://data.x.ai/2025-08-20-grok-4-model-card.pdf>.
- Xie, Z., Cohn, T., and Lau, J. H. The next chapter: A study of large language models in storytelling. *arXiv preprint arXiv:2301.09790*, 2023.
- Xu, H., Wang, D., Zhao, Z., and Yu, Y. Change-point inference in high-dimensional regression models under temporal dependence. *The Annals of Statistics*, 52(3):999–1026, 2024.
- Yang, X., Cheng, W., Wu, Y., Petzold, L. R., Wang, W. Y., and Chen, H. DNA-GPT: Divergent N-gram analysis for training-free detection of GPT-generated text. In *The Twelfth International Conference on Learning Representations*, 2024.
- Yu, X., Qi, Y., Chen, K., Chen, G., Yang, X., Zhu, P., Shang, X., Zhang, W., and Yu, N. DPIC: Decoupling prompt and intrinsic characteristics for llm generated text detection. In Globerson, A., Mackey, L., Belgrave, D., Fan, A., Paquet, U., Tomczak, J., and Zhang, C. (eds.), *Advances in Neural Information Processing Systems*, volume 37, pp. 16194–16212. Curran Associates, Inc., 2024.
- Yu, Y. A review on minimax rates in change point detection and localisation. *arXiv preprint arXiv:2011.01857*, 2020.
- Zeng, Z., Liu, S., Sha, L., Li, Z., Yang, K., Liu, S., Gašević, D., and Chen, G. Towards detecting ai-generated text within human-ai collaborative hybrid texts. *arXiv preprint arXiv:2403.03506*, 2024a.
- Zeng, Z., Liu, S., Sha, L., Li, Z., Yang, K., Liu, S., Gašević, D., and Chen, G. Detecting AI-generated sentences in human-AI collaborative hybrid texts: challenges, strategies, and insights. In *Proceedings of the Thirty-Third International Joint Conference on Artificial Intelligence, IJCAI '24*, 2024b. doi: 10.24963/ijcai.2024/835.
- Zhang, Q., Gao, C., Chen, D., Huang, Y., Huang, Y., Sun, Z., Zhang, S., Li, W., Fu, Z., Wan,

- Y., and Sun, L. LLM-as-a-coauthor: Can mixed human-written and machine-generated text be detected? In Duh, K., Gomez, H., and Bethard, S. (eds.), *Findings of the Association for Computational Linguistics: NAACL 2024*, pp. 409–436, Mexico City, Mexico, June 2024a. Association for Computational Linguistics.
- Zhang, Z., Qin, W., and Plummer, B. Machine-generated text localization. In Ku, L.-W., Martins, A., and Srikumar, V. (eds.), *Findings of the Association for Computational Linguistics: ACL 2024*, pp. 8357–8371, Bangkok, Thailand, August 2024b. Association for Computational Linguistics.
- Zhou, H., Zhu, J., Su, P., Ye, K., Yang, Y., Gavioli-Akilagun, S. A. O. B., and Shi, C. AdadetectGPT: Adaptive detection of LLM-generated text with statistical guarantees. In *The Thirty-ninth Annual Conference on Neural Information Processing Systems*, 2025.
- Zhou, H., Zhu, J., Yang, Y., and Shi, C. Detecting LLM-generated text with performance guarantees. *arXiv preprint arXiv:2601.06586*, 2026a.
- Zhou, H., Zhu, J., Ye, K., Yang, Y., Xu, E., and Shi, C. Learn-to-distance: Distance learning for detecting LLM-generated text. In *The Fourteenth International Conference on Learning Representations*, 2026b.

# A Proofs

## A.1 Assumptions

We list the assumptions required for Theorem 1 and Theorem 2 to hold here. The  $\psi_2$ -norm for sub-Gaussian random variables is defined in (9).

- (i)  $\phi(X_1), \phi(X_2), \dots, \phi(X_N)$  are independent;
- (ii)  $\|\phi(X_i) - \mathbb{E}(\phi(X_i))\|_{\psi_2} \leq \sigma_i$  for all  $i \in [N]$ ;
- (iii) the input threshold  $r$  in Algorithm 1 is set to be proportional to  $\sqrt{\log(N/\delta)}$ ;
- (iv) there exists some sufficiently large constant  $C > 0$  such that the number of random intervals  $M \geq CN^2\Delta_1^{-2} \log(N(\delta\Delta_1)^{-1})$ .

We note that the independence and sub-Gaussianity assumptions, (i) and (ii), are primarily imposed to simplify the theoretical analysis and are standard in the change point detection literature (e.g., Wang et al., 2020; Baranowski et al., 2019; Verzelen et al., 2023). Meanwhile, they can be relaxed to accommodate temporally dependent sequences (e.g., Madrid Padilla et al., 2023; Xu et al., 2024) and heavy-tailed distributions (e.g., Li & Yu, 2021; Cho & Kirch, 2022). We do not further pursue those directions as the main contribution is to understand the effects of heterogeneous  $\sigma_i$  on the signal-to-noise condition and localization error. Assumptions (iii) and (iv) are mild as both  $r$  and  $M$  are user-specified.

## A.2 Proofs for Theorems 1–3

For a real-valued random variable  $X$ , we define its Orlicz- $\psi_2$  norm as

$$\|X\|_{\psi_2} = \inf\{t > 0 : \mathbb{E}[\exp(\{|X|/t\}^2)] \leq 2\}. \quad (9)$$

A variable with a finite Orlicz- $\psi_2$  norm is sub-Gaussian, meaning its distribution has a tail that is at least as light as that of a Gaussian variable.

In this section, we collect the proofs of results in the main sections. To simplify notation, we shall use  $\mathbf{Y} = (Y_1, \dots, Y_N)$  to denote  $\phi(\mathbf{X}) = (\phi(X_1), \dots, \phi(X_N))$ , and use  $\mu = (\mu_1, \dots, \mu_N)$  to denote the mean vector of  $\mathbf{Y}$ . We can further write  $Y_i = \mu_i + \epsilon_i$  where each  $\epsilon_i$  satisfies  $\|\epsilon_i\|_{\psi_2} \leq \sigma_i$ . We also introduce the following general notation. Recall that for a general weight vector  $w = (w_1, \dots, w_N)$ ,  $S_{u:v}^w = \sum_{i=u}^v w_i$ ,  $1 \leq u \leq v \leq N$ . For vectors  $v, w \in \mathbb{R}^N$ , and  $b \in [N]$ , with  $1 \leq s \leq b \leq e-1 < N$ , we write

$$W_{s,e}^v(b) = \sqrt{\frac{S_{s:b}^w S_{(b+1):e}^w}{S_{s:e}^w}} \left| \sum_{i=s}^b \frac{w_i}{S_{s:b}^w} v_i - \sum_{i=b+1}^e \frac{w_i}{S_{(b+1):e}^w} v_i \right| = |\langle v, \psi_{s,e}^b \rangle_w|, \quad (10)$$

where

$$\psi_{s,e}^b(i) = \begin{cases} \sqrt{\frac{S_{(b+1):e}^w}{S_{s:b}^w S_{s:e}^w}}, & s \leq i \leq b, \\ -\sqrt{\frac{S_{s:b}^w}{S_{s:e}^w S_{(b+1):e}^w}}, & b < i \leq e, \\ 0, & \text{otherwise,} \end{cases}$$

and  $\langle x, y \rangle_w = \sum_{i=1}^N x_i y_i w_i$  for two vectors  $x, y \in \mathbb{R}^N$ . We also denote  $\|x\|_w^2 = \langle x, x \rangle_w = x^\top W x$ , with  $W = \text{diag}(w)$ .

The following lemma is important in the proof of Theorem 2.

**Lemma 5.** *Let  $\boldsymbol{\mu} = (\mu_1, \dots, \mu_N)$  denote the mean vector of  $\mathbf{Y} = (Y_1, \dots, Y_N)$  and let  $\tau_1, \dots, \tau_K$  be the change points. Suppose  $1 \leq s < e \leq N$ , such that  $\tau_{j-1} < s \leq \tau_j < e \leq \tau_{j+1}$  for some  $j = 1, \dots, K$ . Let  $\eta = \min\{S_{s:\tau_j}^w, S_{(\tau_j+1):e}^w\}$  and  $\kappa = |\mu_h - \mu_m|$ . Then*

$$W_{s,e}^\mu(\tau_j) = \max_{s \leq b < e} W_{s,e}^\mu(b),$$

and  $\sqrt{\eta}\kappa/\sqrt{2} \leq W_{s,e}^\mu(\tau_j) \leq \sqrt{\eta}\kappa$ . Moreover, it holds that

$$\|\psi_{s,e}^b \langle \psi_{s,e}^b, \boldsymbol{\mu} \rangle_w - \psi_{s,e}^{\tau_j} \langle \psi_{s,e}^{\tau_j}, \boldsymbol{\mu} \rangle_w\|_w^2 = (W_{s,e}^\mu(\tau_j))^2 - (W_{s,e}^\mu(b))^2, \quad (11)$$

and

$$(W_{s,e}^\mu(\tau_j))^2 - (W_{s,e}^\mu(b))^2 = \begin{cases} \frac{S_{(b+1):\tau_j}^w S_{(\tau_j+1):e}^w}{S_{(b+1):e}^w} \kappa^2 & \text{if } s \leq b < \tau_j, \\ \frac{S_{(\tau_j+1):b}^w S_{s:\tau_j}^w}{S_{s:b}^w} \kappa^2 & \text{if } \tau_j \leq b < e. \end{cases} \quad (12)$$

*Proof of Lemma 5.* For a general triplet  $s \leq b < e$ , it holds that

$$W_{s,e}^\mu(b) = \begin{cases} \kappa \sqrt{\frac{S_{s:b}^w}{S_{s:e}^w S_{(b+1):e}^w}} S_{(\tau_j+1):e}^w, & b \leq \tau_j; \\ \kappa \sqrt{\frac{S_{s:\tau_j}^w S_{(\tau_j+1):e}^w}{S_{s:e}^w}}, & b = \tau_j; \\ \kappa \sqrt{\frac{S_{(b+1):e}^w}{S_{s:e}^w S_{s:b}^w}} S_{s:\tau_j}^w, & b \geq \tau_j, \end{cases} \quad (13)$$

and then it is clear that  $W_{s,e}^\mu(b)$  is maximized at  $b = \tau_j$  since all  $w_i \geq 0$  for  $i \in [N]$ . Note that

$$\sqrt{\eta/2} \leq \sqrt{\frac{S_{s:\tau_j}^w S_{(\tau_j+1):e}^w}{S_{s:e}^w}} \leq \sqrt{\eta},$$

which leads to the fact that  $\sqrt{\eta}\kappa/\sqrt{2} \leq W_{s,e}^\mu(\tau_j) \leq \sqrt{\eta}\kappa$ . The expression for  $(W_{s,e}^\mu(\tau_j))^2 - (W_{s,e}^\mu(b))^2$  in (12) follows from direct calculation using (13). Finally, to see (11), we consider first the case  $b < \tau_j$ , then

$$\|\psi_{s,e}^b \langle \psi_{s,e}^b, \boldsymbol{\mu} \rangle_w - \psi_{s,e}^{\tau_j} \langle \psi_{s,e}^{\tau_j}, \boldsymbol{\mu} \rangle_w\|_w^2 = \sum_{i=s}^e w_i k_i^2 \quad (14)$$

where

$$k_i = \begin{cases} \sqrt{\frac{S_{(b+1):e}^w}{S_{s:b}^w S_{s:e}^w}} \langle \psi_{s,e}^b, \boldsymbol{\mu} \rangle_w - \sqrt{\frac{S_{(\tau_j+1):e}^w}{S_{s:\tau_j}^w S_{s:e}^w}} \langle \psi_{s,e}^{\tau_j}, \boldsymbol{\mu} \rangle_w, & s \leq i \leq b; \\ -\sqrt{\frac{S_{s:b}^w}{S_{s:e}^w S_{(b+1):e}^w}} \langle \psi_{s,e}^b, \boldsymbol{\mu} \rangle_w - \sqrt{\frac{S_{(\tau_j+1):e}^w}{S_{s:\tau_j}^w S_{s:e}^w}} \langle \psi_{s,e}^{\tau_j}, \boldsymbol{\mu} \rangle_w, & b < i \leq \tau_j; \\ -\sqrt{\frac{S_{s:b}^w}{S_{s:e}^w S_{(b+1):e}^w}} \langle \psi_{s,e}^b, \boldsymbol{\mu} \rangle_w + \sqrt{\frac{S_{s:\tau_j}^w}{S_{s:e}^w S_{(\tau_j+1):e}^w}} \langle \psi_{s,e}^{\tau_j}, \boldsymbol{\mu} \rangle_w, & \tau_j < i \leq e. \end{cases}$$

Under the observation (10), we can compute  $\langle \psi_{s,e}^{\tau_j}, \boldsymbol{\mu} \rangle_w$  and  $\langle \psi_{s,e}^b, \boldsymbol{\mu} \rangle_w$  using (13) which yields

$$k_i = \begin{cases} 0, & s \leq i \leq b; \\ \kappa^2 \frac{(S_{(\tau_j+1):e}^w)^2}{(S_{(b+1):e}^w)^2} S_{(b+1):\tau_j}^w, & b < i \leq \tau_j; \\ \kappa^2 \frac{S_{(\tau_j+1):e}^w}{(S_{(b+1):e}^w)^2} (S_{(b+1):\tau_j}^w)^2, & \tau_j < i \leq e. \end{cases}$$

Substituting the above in (14) leads to the claimed result when  $b < \tau_j$ . The other case can be obtained in the same way.  $\square$

We first present the proof of Theorem 2 and then comment on how Theorem 1 directly follows from it.

*Proof of Theorem 2.* We follow the structure of the proof of Theorem 1 in Baranowski et al. (2019), which consists of *Five Steps*, and make the necessary changes to accommodate the heterogeneity of  $\sigma_i$  and our **WCP** algorithm. We need to modify the events considered in their *Steps One and Two* as follows. Let  $\boldsymbol{\mu}_\psi = \psi_{s,e}^b \langle \psi_{s,e}^b, \boldsymbol{\mu} \rangle_w - \psi_{s,e}^{\tau_j} \langle \psi_{s,e}^{\tau_j}, \boldsymbol{\mu} \rangle_w$  and

$$\mathcal{D} = \{(j, s, e, b) : j = 1, \dots, K, \tau_{j-1} < s \leq \tau_j, \tau_j < e \leq \tau_{j+1}, s \leq b < e\}.$$

Consider the following two events:

$$\begin{aligned} A &= \left\{ \max_{s,b,e:1 \leq s \leq b < e \leq N} |W_{s,e}^\epsilon(b)| \leq r \right\}, \\ B &= \left\{ \frac{|\langle \boldsymbol{\mu}_\psi, \boldsymbol{\epsilon} \rangle_w|}{\|\boldsymbol{\mu}_\psi\|_w} \leq r, \forall (j, s, e, b) \in \mathcal{D} \right\}. \end{aligned} \tag{15}$$

Note that using independence and sub-Gaussianity of the components of  $\boldsymbol{\epsilon}$  with  $\|\epsilon_i\|_{\psi_2} \leq \sigma_i = w_i^{-1/2}$ , we have

$$\|\langle \boldsymbol{\epsilon}, \psi_{s,e}^b \rangle_w\|_{\psi_2}^2 = \left\| \sum_{i=1}^N w_i \epsilon_i \psi_{s,e}^b(i) \right\|_{\psi_2}^2 \leq C \sum_{i=1}^N \left\| w_i \epsilon_i \psi_{s,e}^b(i) \right\|_{\psi_2}^2 \leq C,$$

for some absolute constant  $C$ , where the first inequality is due to Proposition 2.7.1 in Vershynin (2018). Similarly, it also holds that

$$\left\| \frac{\langle \boldsymbol{\mu}_\psi, \boldsymbol{\epsilon} \rangle_w}{\|\boldsymbol{\mu}_\psi\|_w} \right\|_{\psi_2} \leq C.$$

Hence, using a union bound and tail bound for sub-Gaussian random variable (e.g. Vershynin, 2018, Proposition 2.6.6), we obtain

$$\mathbb{P}(A^c) \leq N^3 \exp(-cr^2) \quad \mathbb{P}(B^c) \leq N^4 \exp(-cr^2).$$

Choosing  $r = c' \sqrt{\log(N/\delta)}$  with a large enough absolute constant  $c' > 0$  ensures both  $\mathbb{P}(A^c)$  and  $\mathbb{P}(B^c)$  are less than  $\delta$ .

*Step Three* is the key step showing the difference between the signal-to-noise conditions (4) and (7). The main goal of this step is to show that when a large number of random intervals are generated, each change point  $\tau_j$  is captured by some interval. However, under different conditions, we need to consider intervals at different “scales.”

**Under the signal-to-noise condition in (4), i.e.**

$$(\mu_m - \mu_h)^2 \Delta_1 \gtrsim \sigma_{\max}^2 \log(N/\delta) = \frac{\log(N/\delta)}{\min_{i \in [N]} w_i},$$

where  $\Delta_1 = \min_{j \in [K+1]} \{\tau_j - \tau_{j-1}\}$ , we can consider intervals directly at the index scale, as in the proof of Theorem 1 in Baranowski et al. (2019). Let

$$\mathcal{I}_j^L = (\tau_j - \Delta_1/3, \tau_j - \Delta_1/6) \quad \mathcal{I}_j^R = (\tau_j + \Delta_1/6, \tau_j + \Delta_1/3),$$

and  $\mathcal{M} = \{[s_1, e_1], \dots, [s_M, e_M]\}$  be the randomly generated intervals. The following event

$$C = \{\forall j = 1 \dots, K, \exists m \in \{1, \dots, M\}, \text{s.t. } s_m \in \mathcal{I}_j^L, e_m \in \mathcal{I}_j^R\},$$

satisfies

$$\mathbb{P}(C) \geq 1 - \delta \quad \text{if } M \geq 36N^2 \Delta_1^{-2} \log(N(\delta \Delta_1)^{-1}),$$

using the arguments in the original proof.

**Under the signal-to-noise condition in (7), i.e.**

$$(\mu_m - \mu_h)^2 \Delta_2 \gtrsim \log(N/\delta),$$

where  $\Delta_2 = \min_{j \in [K+1]} S_{(\tau_{j-1}+1):\tau_j}^w = \min_{j \in [K+1]} \sum_{i=\tau_{j-1}+1}^{\tau_j} \sigma_i^{-2}$ , we need to adapt the lengths of  $\mathcal{I}_j^L$  and  $\mathcal{I}_j^R$  to the scale of the weights. Specifically, with a slight abuse of notation we again let

$$\begin{aligned} \mathcal{I}_j^L &= \{s \in \{1, \dots, \tau_j\} : \Delta_2/6 < S_{s:\tau_j}^w < \Delta_2/3\}, \\ \mathcal{I}_j^R &= \{e \in \{\tau_j + 1, \dots, N\} : \Delta_2/6 < S_{(\tau_j+1):e}^w < \Delta_2/3\}. \end{aligned} \tag{16}$$

Note that the set  $\mathcal{I}_j^L$  will not include any points  $i \leq \tau_{j-1}$  since  $S_{(\tau_{j-1}+1):\tau_j}^w \geq \Delta_2$ . Similarly,  $\mathcal{I}_j^R$  will also not include any points  $i > \tau_{j+1}$ . Moreover, these two sets are non-empty since  $\max_{i \in [N]} w_i < \Delta_2/6$  by assumption, so that each set contains at least one element. Again, we let  $[s_1, e_1], \dots, [s_M, e_M]$  be the randomly generated intervals and consider event  $C$  as above. Note that for each interval  $[s_m, e_m]$ , we have  $\mathbb{P}(s_m \in \mathcal{I}_j^L, e_m \in \mathcal{I}_j^R) \geq 1/N^2$ . Then, we can control

$$\mathbb{P}(C^c) \leq \sum_{j=1}^K \prod_{m=1}^M (1 - \mathbb{P}(s_m \in \mathcal{I}_j^L, e_m \in \mathcal{I}_j^R)) \leq K \left(1 - \frac{1}{N^2}\right)^M \leq K \exp(-M/N^2).$$

Therefore, choosing  $M \geq N^2 \log(K/\delta)$  ensures

$$\mathbb{P}(C) \geq 1 - \delta.$$

In the following, we work under the event  $A \cap B \cap C$ , which happens with probability at least  $1 - 3\delta$ .

In *Step Four*, we aim to find an upper bound on the localization error. Consider the set of over-thresholding intervals

$$\mathcal{O} = \{m \in \mathcal{M} : \max_{s_m \leq b < e_m} W_{s_m, e_m}^{\mathbf{Y}}(b) > r\}.$$

Using the event  $A$  and Lemma 5, we have that this set is non-empty under the weaker signal-to-noise condition (7). Therefore it is also non-empty under the condition (4) since

$$\Delta_2 = \min_{j \in [K+1]} \sum_{i=\tau_{j-1}+1}^{\tau_j} \frac{1}{\sigma_i^2} \geq \frac{\Delta_1}{\sigma_{\max}^2}.$$

There is a slight difference in how we select the shortest over-threshold interval, depending on whether we work under the condition (4) or (7). This is related to the fact that the intervals are defined at different scales. In particular, we choose  $m^* = \arg \min_{m \in \mathcal{O}} (e_m - s_m + 1)$  when assuming (4) and  $m^* = \arg \min_{m \in \mathcal{O}} (S_{(s_m+1):e_m}^w)$  when assuming (7). Such choices ensure that the corresponding intervals cannot contain more than one change point.

With a slight abuse of notation, we simply use  $[s, e]$  to denote the interval  $[s_{m^*}, e_{m^*}]$ . It can be shown using the same arguments as in Baranowski et al. (2019) that this interval contains a single change point, which we denote as  $\tau_j$ , and  $\min\{S_{s:\tau_j}^w, S_{(\tau_j+1):e}^w\} > r^2/\kappa^2$ . The estimator is  $\hat{\tau}_j = \hat{b} = \arg \max_{b \in [s, e]} W_{s, e}^{\mathbf{Y}}(b)$ . The arguments below do not rely on the signal-to-noise conditions. To control the error between  $\tau_j$  and  $\hat{b}$ , note that

$$\begin{aligned} (W_{s, e}^{\mathbf{Y}}(\tau_j))^2 - (W_{s, e}^{\mathbf{Y}}(b))^2 &= (\langle \mathbf{Y}, \psi_{s, e}^{\tau_j} \rangle_w)^2 - (\langle \mathbf{Y}, \psi_{s, e}^b \rangle_w)^2 \\ &= (\langle \boldsymbol{\mu}, \psi_{s, e}^{\tau_j} \rangle_w)^2 - (\langle \boldsymbol{\mu}, \psi_{s, e}^b \rangle_w)^2 + (\langle \boldsymbol{\epsilon}, \psi_{s, e}^{\tau_j} \rangle_w)^2 - (\langle \boldsymbol{\epsilon}, \psi_{s, e}^b \rangle_w)^2 \\ &\quad + 2\langle \boldsymbol{\epsilon}, \psi_{s, e}^{\tau_j} \langle \psi_{s, e}^{\tau_j}, \boldsymbol{\mu} \rangle_w - \psi_{s, e}^b \langle \psi_{s, e}^b, \boldsymbol{\mu} \rangle_w \rangle. \end{aligned}$$

Consider first  $b \geq \tau_j$ , and the other case can be dealt with similarly. Using Lemma 5 together with the identity (10), we have

$$(\langle \boldsymbol{\mu}, \psi_{s, e}^{\tau_j} \rangle_w)^2 - (\langle \boldsymbol{\mu}, \psi_{s, e}^b \rangle_w)^2 = \frac{S_{(\tau_j+1):b}^w S_{s:\tau_j}^w}{S_{s:b}^w} \kappa^2.$$

Using the bounds in events  $A$  and  $B$  (15), we further have

$$\begin{aligned} (\langle \boldsymbol{\epsilon}, \psi_{s, e}^{\tau_j} \rangle_w)^2 - (\langle \boldsymbol{\epsilon}, \psi_{s, e}^b \rangle_w)^2 &\leq r^2 \\ 2\langle \boldsymbol{\epsilon}, \psi_{s, e}^{\tau_j} \langle \psi_{s, e}^{\tau_j}, \boldsymbol{\mu} \rangle_w - \psi_{s, e}^b \langle \psi_{s, e}^b, \boldsymbol{\mu} \rangle_w \rangle &\leq 2r \|\psi_{s, e}^{\tau_j} \langle \psi_{s, e}^{\tau_j}, \boldsymbol{\mu} \rangle_w - \psi_{s, e}^b \langle \psi_{s, e}^b, \boldsymbol{\mu} \rangle_w\|_w \\ &= 2r \sqrt{\frac{S_{(\tau_j+1):b}^w S_{s:\tau_j}^w}{S_{s:b}^w}} \kappa. \end{aligned}$$

Notice that if

$$\frac{2S_{(\tau_j+1):b}^w S_{s:\tau_j}^w}{S_{s:b}^w} \kappa^2 = \frac{2(S_{s:b}^w - S_{s:\tau_j}^w) S_{s:\tau_j}^w}{S_{s:b}^w} \kappa^2 \geq \min\{S_{s:\tau_j}^w, S_{(\tau_j+1):b}^w\} \kappa^2 > r^2,$$

then  $(W_{s,e}^Y(\tau_j))^2 - (W_{s,e}^Y(b))^2 > 0$ . Since  $S_{s:\tau_j}^w > r^2/\kappa^2$ , we have that the estimator  $\hat{b}$  must satisfy

$$S_{(\tau_j+1):\hat{b}}^w = \sum_{i=\tau_j+1}^{\hat{b}} w_i = \sum_{i=\tau_j+1}^{\hat{b}} \frac{1}{\sigma_i^2} \leq \frac{r^2}{\kappa^2},$$

as, otherwise, it cannot be the maximizer of  $W_{s,e}^Y(b)$ . For  $b < \tau_j$ , following the same arguments and using the fact  $S_{(\tau_j+1):e}^w > r^2/\kappa^2$ , we would obtain

$$\sum_{\hat{b}+1}^{\tau_j} \frac{1}{\sigma_i^2} \leq \frac{r^2}{\kappa^2}.$$

Therefore, combining these two cases, we obtain

$$\sum_{\min\{\tau_j, \hat{b}\}+1}^{\max\{\tau_j, \hat{b}\}} \frac{1}{\sigma_i^2} \leq \frac{r^2}{\kappa^2}.$$

Finally, we note that we omit the details of Step Five, which deals with the recursive aspect of the algorithm and shows that the true number of change points  $K$  is recovered. This step in our case follows directly by using similar adjustments to the intervals  $[s_k, e_k]$  as (16), and incurring a slightly modified version of Lemma 3 in Baranowski et al. (2019) with  $\tau_j - s + 1$  replaced by  $S_{s:\tau_j}^w$  and  $e - \tau_j$  replaced by  $S_{(\tau_j+1):e}^w$ .  $\square$

*Proof of Theorem 1.* Note that as long as  $w_i = c$  for some  $c > 0$ , it holds that

$$\begin{aligned} W_{s,e}^v(b) &= \sqrt{\frac{S_{s:b}^w S_{(b+1):e}^w}{S_{s:e}^w}} \left| \sum_{i=s}^b \frac{w_i}{S_{s:b}^w} v_i - \sum_{i=b+1}^e \frac{w_i}{S_{(b+1):e}^w} v_i \right| \\ &= \sqrt{c} \sqrt{\frac{(b-s+1)(e-b)}{e-s+1}} \left| \frac{\sum_{i=s}^b v_i}{b-s+1} - \frac{\sum_{i=b+1}^e v_i}{e-b} \right| = \sqrt{c} C_{s,e}^v(b). \end{aligned}$$

Moreover, choosing  $c = 1/\sigma_{\max}^2 = \min_{i \in [N]} w_i$  ensures that the high-probability events  $A$  and  $B$  in the proof of Theorem 2 still hold with the same choice of  $r$ . Therefore the conclusion of Theorem 2 still holds but only with  $w_i = 1/\sigma_{\max}^2$ . Substituting this choice into the bound (6), we obtain the claimed result

$$\max_{j \in [K]} |\hat{\tau}_j - \tau_j| \lesssim \frac{\sigma_{\max}^2 \log(N/\delta)}{(\mu_m - \mu_h)^2}.$$

$\square$

*Proof of Theorem 3.* Fix a  $\delta \in (0, 1/2)$ . We start by considering the following two distributions

$P_1$  and  $P_2$  both belonging to  $\mathcal{P}$ , where  $P_1$  is the joint distribution  $N$  independent random variables such that

$$Y_i \sim N(\mu_m, \sigma_i^2) \quad i \leq \tau, \quad Y_i \sim N(\mu_h, \sigma_i^2) \quad i > \tau.$$

$P_2$  denotes the joint distribution  $N$  independent random variables such that

$$Y_i \sim N(\mu_m, \sigma_i^2) \quad i \leq \tau + h_1, \quad Y_i \sim N(\mu_h, \sigma_i^2) \quad i > \tau + h_1.$$

Let  $\kappa = |\mu_m - \mu_h|$  and then  $D_{\text{KL}}(P_1, P_2) = \sum_{i=\tau+1}^{\tau+h_1} \frac{\kappa^2}{\sigma_i^2}$ . Now, applying [Ma et al. \(2024, Corollary 6\)](#), a version of Le Cam's two-point lemma for high-probability lower bounds, we obtain that if  $h_1$  is chosen such that

$$\sum_{i=\tau+1}^{\tau+h_1} \frac{\kappa^2}{\sigma_i^2} \leq \log\left(\frac{1}{4\delta(1-\delta)}\right),$$

then  $\inf_{\hat{\tau}} \sup_{P \in \mathcal{P}} Q(\delta, \hat{\tau}, P) \gtrsim h_1$ . Therefore, we can choose it to be  $\max\{h_1 \in [N - \tau] : \sum_{i=\tau+1}^{\tau+h_1} \frac{\kappa^2}{\sigma_i^2} \leq \log(\frac{1}{4\delta(1-\delta)})\}$  and this value is guaranteed to be less than  $N - \tau$  since  $\kappa^2 S_{(\tau+1):N}^w \gtrsim \log(1/\delta)$ , as required in  $\mathcal{P}$ . The other lower bound can be obtained by considering  $P_1$  and  $P_3$  belonging to  $\mathcal{P}$ , where  $P_3$  is the joint distribution of  $N$  independent random variables such that

$$Y_i \sim N(\mu_m, \sigma_i^2) \quad i \leq \tau - h_2 - 1, \quad Y_i \sim N(\mu_h, \sigma_i^2) \quad i \geq \tau - h_2.$$

Then we have  $D_{\text{KL}}(P_1, P_3) = \sum_{i=\tau-h_2}^{\tau} \frac{\kappa^2}{\sigma_i^2}$ . The same arguments as before implies that if  $h_2$  satisfies

$$\sum_{i=\tau-h_2}^{\tau} \frac{\kappa^2}{\sigma_i^2} \leq \log\left(\frac{1}{4\delta(1-\delta)}\right),$$

then  $\inf_{\hat{\tau}} \sup_{P \in \mathcal{P}} Q(\delta, \hat{\tau}, P) \gtrsim h_2$ . We take  $\max\{h_2 \in [\tau] : \sum_{i=\tau-h_2}^{\tau} \frac{\kappa^2}{\sigma_i^2} \leq \log(\frac{1}{4\delta(1-\delta)})\}$  and this value is guaranteed to be less than  $\tau$  since  $\kappa^2 S_{1:\tau}^w \gtrsim \log(1/\delta)$ , as required in  $\mathcal{P}$ . Combining these two cases yields our claim.  $\square$

### A.3 Equivalence of GCP and WCP

In this section, we show the equivalence between (3) and (2) when  $\phi$  takes certain general forms that are used in the literature (e.g. [Mitchell et al., 2023](#); [Bao et al., 2024](#); [Zhou et al., 2025](#)). Let  $Z_t = \mathcal{R}(X_t)$  denote the text rewritten by some LLM given input text  $X_t$ ,  $X_{t,i}$  denote the  $i$ -th token in the  $t$ -th sentence, and  $X_{t,<i}$  denote all the tokens before  $i$ -th token in the  $t$ -th sentence. Assume  $Y_t$  and  $X_t$  share the same number of tokens  $n_t$ , which can be achieved by zero-padding the shorter sequence. Consider the detector  $\phi$  that takes the form of either a zero-shot detection statistic

$$\phi_1(X_t) = \frac{1}{n_t} \log p_{\hat{\varphi}}(X_t),$$

where  $p_{\hat{\varphi}}$  is some possible source model to be detected, or a ML-based detection statistic

$$\phi_2(X_t) = \frac{1}{n_t} \log \frac{p_{\hat{\varphi}}(X_t)}{p_{\hat{\varphi}}(Z_t)} = \frac{1}{n_t} \sum_{i=1}^{n_t} \log \frac{p_{\hat{\varphi}}(X_{t,i} | X_{t,<i})}{p_{\hat{\varphi}}(Z_{t,i} | Z_{t,<i})},$$

where  $p_{\hat{\varphi}}$  is a classifier trained to maximally distinguish  $X_t$  and  $Z_t$ .

**Proposition 6.** *Under the above choices of detection statistics  $\phi$ , if for any input text  $\mathbf{X}$  with  $N$  sentences, where each sentence  $X_i$  has  $n_i$  tokens, it holds that*

$$p_{\hat{\varphi}}(X_{i,j}|X_{i,<j}) = p_{\hat{\varphi}}(X_{i,j}|X_{<i,<j}), \quad (17)$$

for  $i \in [N], j \in [n_i]$ , then

$$G_{s,e}^{\mathbf{X}}(b) = W_{s,e}^{\mathbf{Y}}(b), \quad \forall b \in [N],$$

with  $Y = (\phi(X_1), \dots, \phi(X_N))$  and  $w_i = n_i$ .

*Proof of Proposition 6.* We directly prove the case for  $\phi_2$ , and the case for  $\phi_1$  is a special case by setting  $p_{\hat{\varphi}}(Z_t) = 1$ . Under  $\phi_2$ , we have

$$D_{s,e}^{\mathbf{X}}(b) = \sqrt{\frac{S_{s:b}^w S_{(b+1):e}^w}{S_{s:e}^w}} \left| \frac{1}{S_{s:b}^w} \sum_{i=s}^b \sum_{j=1}^{n_i} \log \frac{p_{\hat{\varphi}}(X_{i,j}|X_{<i,<j})}{p_{\hat{\varphi}}(Z_{i,j}|Z_{<i,<j})} - \frac{1}{S_{(b+1):e}^w} \sum_{i=b+1}^e \sum_{j=1}^{n_i} \log \frac{p_{\hat{\varphi}}(X_{i,j}|X_{<i,<j})}{p_{\hat{\varphi}}(Z_{i,j}|Z_{<i,<j})} \right|$$

$$W_{s,e}^{\mathbf{Y}}(b) = \sqrt{\frac{S_{s:b}^w S_{(b+1):e}^w}{S_{s:e}^w}} \left| \frac{1}{S_{s:b}^w} \sum_{i=s}^b \sum_{j=1}^{n_i} \log \frac{p_{\hat{\varphi}}(X_{i,j}|X_{i,<j})}{p_{\hat{\varphi}}(Z_{i,j}|Z_{i,<j})} - \frac{1}{S_{(b+1):e}^w} \sum_{i=b+1}^e \sum_{j=1}^{n_i} \log \frac{p_{\hat{\varphi}}(X_{i,j}|X_{i,<j})}{p_{\hat{\varphi}}(Z_{i,j}|Z_{i,<j})} \right|$$

Therefore, under the assumption that for any  $i \in [N]$  and  $j \in [n_i]$ ,

$$p_{\hat{\varphi}}(X_{i,j}|X_{i,<j}) = p_{\hat{\varphi}}(X_{i,j}|X_{<i,<j}),$$

where  $X$  is the input text, it holds that  $W_{s,e}^{\mathbf{Y}}(b) = D_{s,e}^{\mathbf{X}}(b)$  for all  $b \in [N]$ .  $\square$

## B Additional numerical results

### B.1 Additional experiments with varying detectors

Our method requires a sentence-level detector as input. While the main text uses AdaDetectGPT, here we examine whether the proposed change-point procedure remains effective with alternative detector scores, including log likelihood (LL; Gehrmann et al., 2019), log-likelihood log-rank ratio (LRR; Su et al., 2023), and Fast-DetectGPT (FDGPT; Bao et al., 2024). For a concise comparison, we report SenPred and Voting, which are among the strongest baselines in the main experiments. Table A1 shows that WCP remains competitive across all three detector choices, suggesting that our gain over baselines is not tied to a particular detector.

Table A1: Robustness to different sentence-level detector scores.

Detector	Method	WikiQA		News		Story	
		WD	CE	WD	CE	WD	CE
LL	SenPred	0.57	-1.34	2.85	-11.09	2.38	-9.08
	Voting	0.40	-0.07	0.77	-2.46	0.88	-2.99
	WCP	<b>0.30</b>	<b>-0.05</b>	<b>0.28</b>	<b>-1.18</b>	<b>0.37</b>	<b>-1.94</b>
LRR	SenPred	0.61	-1.57	3.11	-12.31	2.93	-11.98
	Voting	0.43	-0.17	0.96	-3.26	0.92	-3.31
	WCP	<b>0.30</b>	<b>-0.02</b>	<b>0.37</b>	<b>-1.43</b>	<b>0.36</b>	<b>-1.70</b>
FDGPT	SenPred	0.47	-1.26	2.87	-11.19	2.98	-11.79
	Voting	0.39	-0.10	0.59	-1.92	0.85	-3.04
	WCP	<b>0.30</b>	<b>-0.03</b>	<b>0.29</b>	<b>-1.69</b>	<b>0.31</b>	<b>-1.53</b>

## B.2 Additional experiments on token-level detection

We further evaluate the proposed localization idea in a token-level setting, which provides a finer-grained test of mixed human–LLM editing. We consider cases where either 40 or 100 tokens are generated by an LLM. We compare our method with Voting and TokenPred, where TokenPred applies the detection statistic to a 20-token window around each target token before classification. The results in Table A2 show that our method achieves substantially smaller WD and more stable CE, indicating that the change-point formulation remains useful.

Table A2: Token-level localization under different lengths of LLM-generated content.

Number	Methods	WD	CE
40	TokenPred	10.62	-42.58
	Voting	1.127	-4.58
	WCP	<b>0.379</b>	<b>-0.98</b>
100	TokenPred	21.483	-90.818
	Voting	2.611	-9.737
	WCP	<b>0.222</b>	<b>0.172</b>

## C Experiment details

**Implementation details.** For VCP and WCP in the reported experiments, we fix the input parameter  $M$  in Algorithm 1 at 200 and set  $r = \sqrt{\log(N)}$ .

For LLMPred, we use the following prompt to identify LLM-generated segments:

#### Prompt for implementing LLMPred

You are an expert in determining the LLM-written sentences in text. Return ONLY the sentence indices (starting from 0) that are written by a language model.

The text to detect is: [filled in the bracket]. The sentence indices are:

For TextTiling, we use the implementation in `nlk.tokenize.texttiling` (Bird et al., 2009).

For SegFormer in the CoAuthor experiment, we use the implementation provided by Zeng et al. (2024b), which is publicly available on GitHub<sup>2</sup>.

**Human-LLM co-authored text generation procedure.** As mentioned in Section 5, we asked one LLM to rewrite pieces of human-written text to obtain semantically fluent co-authored text. The prompt for generating the LLM-rewritten text is:

#### Prompt on generating the LLM-written text

[System prompt] You are a creative writing assistant. Continue the given text naturally and fluently, matching the style and tone of what came before.

User prompt: Continue the following text by writing approximately {k} more sentences. Return ONLY the new continuation sentences, without repeating the original text.

{preceding text filled in the bracket}

Without loss of generality, we perform sampling with the temperature set to 0.8. Claude 4.5 in the main text corresponds to `claude-haiku-4-5`, and the GPT-5-mini model corresponds to `gpt-5-mini`. All experiments are conducted on an H20 96 GB GPU with 96 Intel(R) Xeon(R) Platinum 8255C CPUs @ 2.50 GHz.

**Settings for LLM detectors.** We consider several LLM detectors: AdaDetectGPT, LL, LRR, and FastDetectGPT. For AdaDetectGPT, its scoring model is a pretrained transformation applied consistently across all experiments. For FastDetectGPT, we set `score` and `sample` to be the same model, chosen from `google/gemma-2-9b-it`. Finally, LL and LRR also require a scoring model, which we set to `google/gemma-2-9b-it`, as in FastDetectGPT.

**Evaluation details.** Let  $C_i^{(r)}$  and  $C_i^{(h)}$  denote the numbers of true and estimated change points

<sup>2</sup>[https://github.com/douglashiwo/AISentenceDetection/blob/main/A-Segment\\_Detection\\_Models/SegFormer.zip](https://github.com/douglashiwo/AISentenceDetection/blob/main/A-Segment_Detection_Models/SegFormer.zip)

in the  $i$ -th sliding window. The WindowDiff metric is defined as:

$$\text{WD} = \frac{1}{T-k} \sum_{i=1}^{T-k} |C_i^{(r)} - C_i^{(h)}|.$$